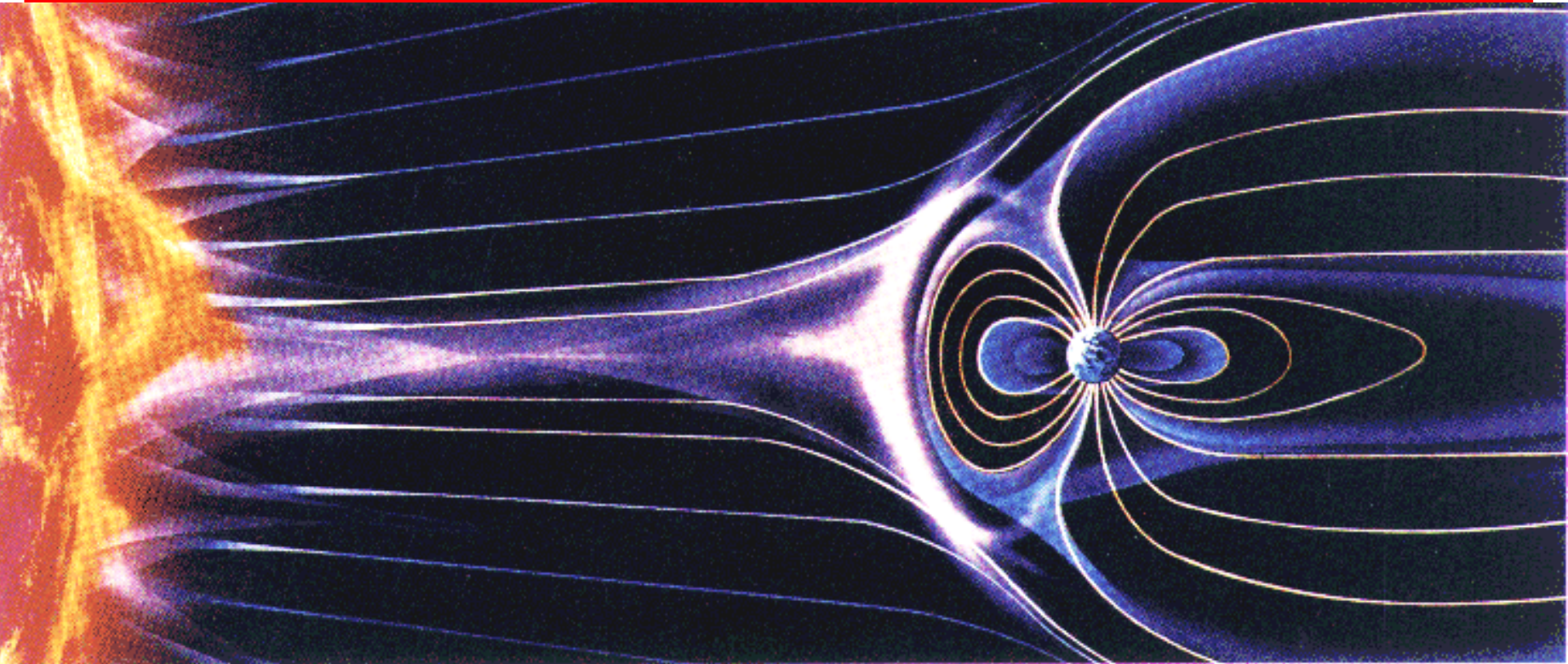




The Solar Wind



Adolfo F.- Viñas

Laboratory for Geospace Physics, NASA/GSFC, Heliosphysics Science
Division - Code 673, Greenbelt, MD 20771, USA, adolfo.vinas@nasa.gov

ISSS/SCOSTEP September 15-19, 2014 Lima, Peru



SW Historical Background - 1

- The Earth's atmosphere is more stationary compared to that at the Sun. The Sun's atmosphere is not stable but is blown out into space as the solar wind filling the solar system.
- The first direct measurements of the solar wind were in the 1960's but it had already been suggested in the early 1900s.
 - To explain a correlation between auroras and sunspots *Birkeland* [1908] suggested continuous corpuscular emission from these spots.
 - Others suggested that particles were emitted from the Sun only during flares and that otherwise space was empty [*Chapman and Ferraro, 1931*].
 - Observations of comet tails lead to the suggestion of a continuous solar wind (Bierman, 1951).
 - The question of a continuous solar wind was resolved in 1962 when the Mariner 2 spacecraft returned 3 months of continuous solar wind data while traveling to Venus.



SW Historical Background - 2

- Bierman, 1951: Cometary tails point directly away from Sun regardless of comet's velocity

To Sun \Rightarrow must be ionized gas pushed away by solar ionized gas, the solar wind



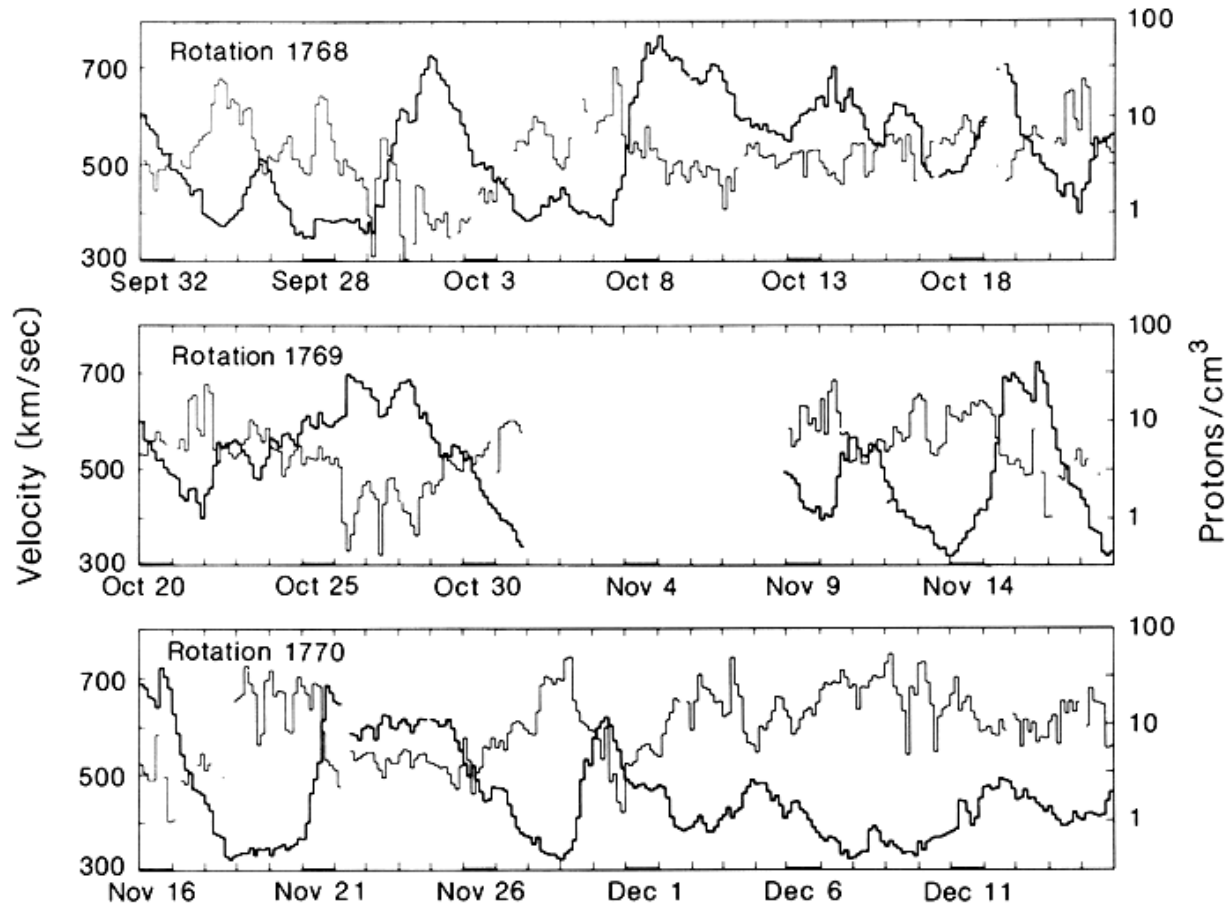
Solar Wind forms the ion tail. Solar wind must have very high speed relative to comet, to align tail with sun direction.

Radiation pressure on micro-size dust grains forms the diffuse dust tail. Grains have less sunward force, move further away from Sun, but fall behind the radial direction because their angular speed is lower than closer in. Dust tails curve around (lag from radial direction).

Image of Hale Bopp Comet



- Measured solar wind speeds (heavy lines) and densities (light lines) with Mariner 2 in 1962 [*Hundhausen, 1995*].





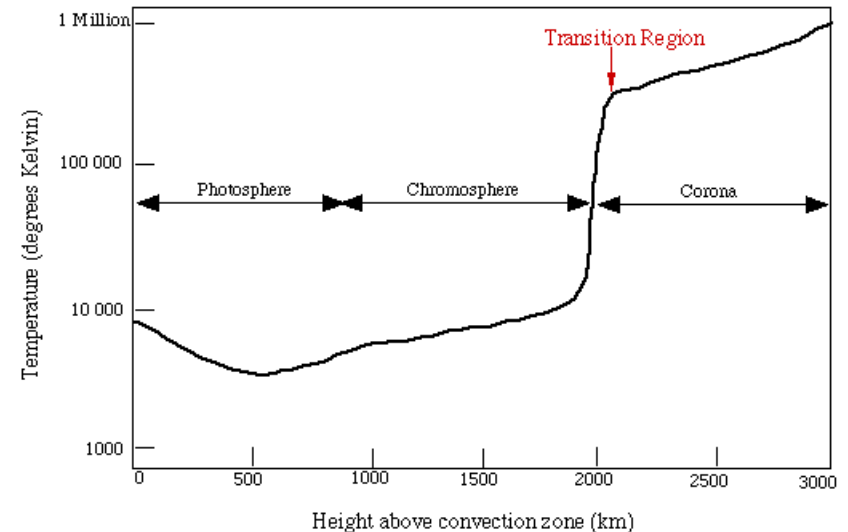
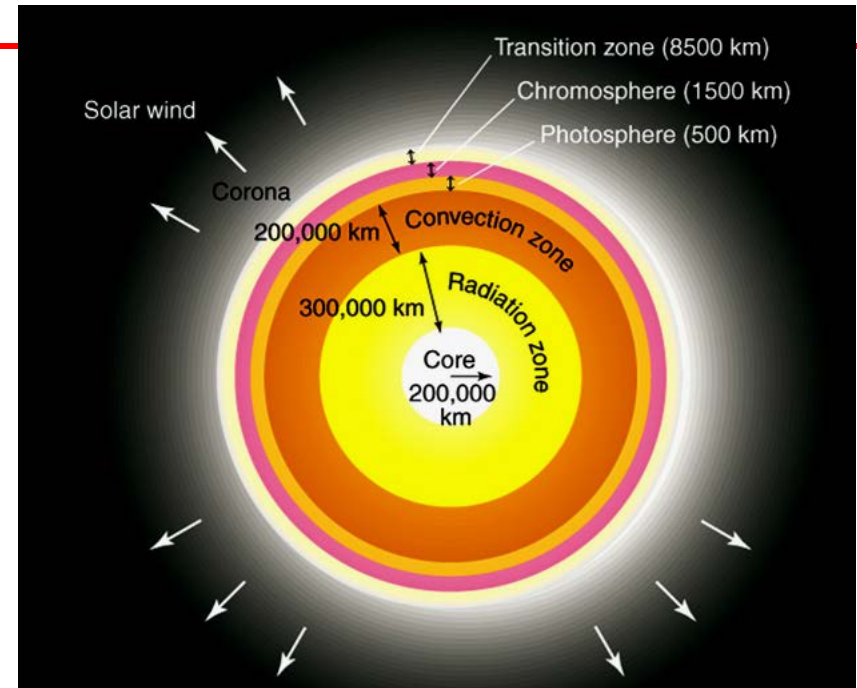
- The most detailed observations of the solar wind have been made from spacecraft near the Earth.

<u>Observed Properties of the Solar Wind near the Orbit of the Earth (1-AU) (after Hundhausen, [1995])</u>	
Proton density	6.6 cm ⁻³
Electron density	7.1 cm ⁻³
He ²⁺ density	0.25 cm ⁻³
Flow speed (nearly radial)	450 km s ⁻¹
Proton temperature	1.2x10 ⁵ K
Electron temperature	1.4x10 ⁵ K
Magnetic field	7x10 ⁻⁹ T



NEAR THE SUN

- The Sun's surface is relatively cool, 5700K compared to the solar wind whose protons have a temperature of about $T_p \sim 1.2 \times 10^5$ K.
- Above the photosphere the temperature first drops and then increases slowly in what it is called the chromosphere.
- Subitely, at about 2000km ($0.003 R_S$) both electrons and ions heats up rapidly.
- What produces such a rapid heating is still controversial. a) Alfvén waves due to the wiggling of magnetic fields below the photosphere?, b) Release of magnetic energy due to reconnection?, c) sound waves?,
?
- d) Other?





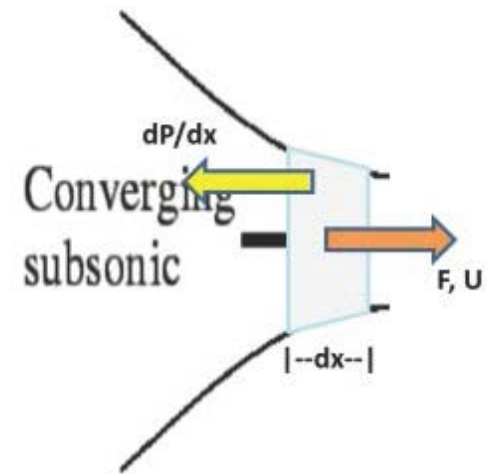
-
- The solar wind exists because the Sun maintains a $2 \times 10^6 \text{K}$ corona as its outer most atmosphere.
 - The Sun's atmosphere "boils off" into space and is accelerated to high velocities ($> 400 \text{ km s}^{-1}$).
 - *Parker* [1958] proposed that the solar wind was the result of the high temperature corona and developed a **hydrodynamic model** to support his idea. Based on this Dessler developed a simple gravitational nozzle which demonstrates the basic physics.
 - Simplifying assumptions:
 1. The solar wind can be treated as an ideal gas.
 2. The solar wind flows radially from the Sun.
 3. Acceleration due to electromagnetic fields is negligible.
 4. The solution is time stationary (i.e. the time scale for solar wind changes is long compared to the time scale for solar wind generation).



Solar Wind Acceleration - 1

Convergent nozzle

The Sun behaves like a rocket engine blasting its exhaust into space. The expansion of the solar corona is similar to that describing the flow of a gas through a nozzle. This is called de Laval Nozzle.



How does supersonic flow occur in a nozzle?

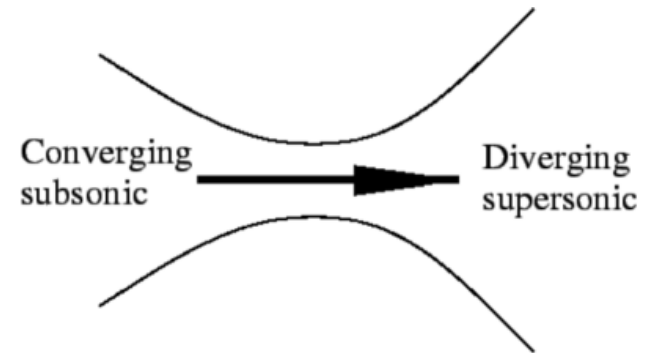
- If we force a gas in a converging nozzle, the flow chokes at the narrowest end. No matter what the pressure differential between the ends of the nozzle is or even if the narrow end exhaust into a vacuum, supersonic flow cannot result. The maximum speed of the flow depends on the pressure differential developed at the narrowest part of the nozzle and it is equal or less than the sound speed.



Solar Wind Acceleration - 2

Whether or not supersonic flow is realized it will depend, of course, on the differential pressure. In a divergent nozzle the flow is also subsonic. This is analogous to a solar corona expansion when gravitational effects are neglected.

deLaval Nozzle



The only way to obtain supersonic flow speed in the steady-state is by a convergent-divergent nozzle as in Figure 2.

Theory: {	In steady-state	
	Mass Conservation	$\rho UA = const.$
	Momentum Conservation	$dP = -\rho U dU$

ρ – density, U – flow speed, A – cross sectional area



Solar Wind Acceleration - 3

Combining Mass and Momentum Conservation

$$\frac{dA}{A} + \frac{d\rho}{\rho} + \frac{dU}{U} = 0$$

$$\frac{dP}{\rho} = \frac{dP}{d\rho} \frac{d\rho}{\rho} = -U dU$$

Specify the physical nature of the process: isothermal or adiabatic

$$\frac{dP}{d\rho} = \begin{cases} = \frac{c_s^2}{\gamma} & \text{adiabatic} \\ = c_s^2 & \text{isothermal} \end{cases}$$

Defining:

$$P = K \rho^\gamma$$

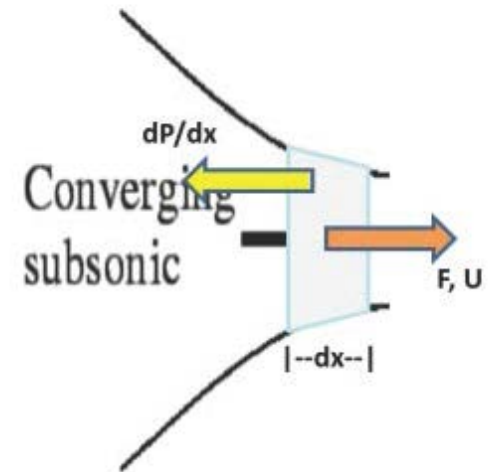
c_s – sound speed



Solar Wind Acceleration - 4

Convergent nozzle

(A) Consider a subsonic flow $\mathbf{U} < \mathbf{c}_s$ in a convergent nozzle as in Fig-1. The bracket in the RHS of (EQ-1) is negative but also the cross-sectional area of the nozzle is decreasing (then $dA < 0$ in the positive direction of the flow), therefore $dU > 0$ and $dU/U > 0$, but since the flow was subsonic, the flow will remain being subsonic.



$$\frac{dA}{A} = \left(\frac{U^2}{c_s^2} - 1 \right) \frac{dU}{U}$$

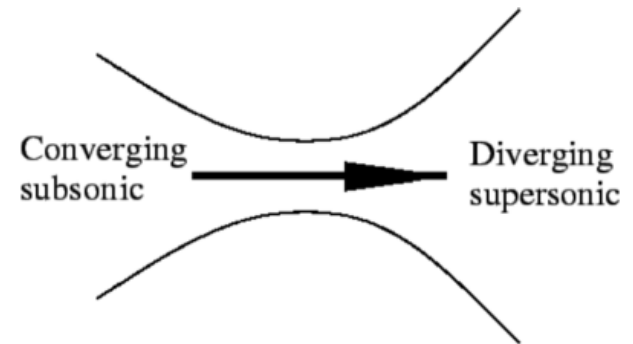
EQ-1



Solar Wind Acceleration - 5

(B) Consider a converging-diverging nozzle as in Fig-2. Suppose again that the flow is subsonic flow ($U < c_s$) then again the term in bracket on (EQ-1) is also negative and also $dA < 0$ and $dA/A < 0$, then $dU > 0$ and also $dU/U > 0$. As we proceed in the direction of the flow we will arrive to the 'neck' where the tube stop converging and the walls of the nozzle are now parallel so that $dA = 0$. This condition can be satisfied if either the bracket in (EQ-1) is zero, i.e. $U = c_s$ or $dU = 0$. When $U = c_s$ this is called the sonic point (i.e. Mach one) . For U to exceed c_s , the tube must diverge so that $dA > 0$ and $U > c_s$ and so $dU/U > 0$. This configuration is called de Laval Nozzle.

deLaval Nozzle



$$\frac{dA}{A} = \left(\frac{U^2}{c_s^2} - 1 \right) \frac{dU}{U}$$

EQ-1



Solar Wind Acceleration - 6

Parker developed the **hydrodynamic** theory of the solar wind and proposed that the solar wind escapes from the solar corona with a velocity changing from subsonic to supersonic speeds.

$$\frac{\partial \rho}{\partial t} + \nabla \cdot (\rho \mathbf{U}) = 0$$

$$\rho \left(\frac{\partial \mathbf{U}}{\partial t} + \mathbf{U} \cdot \nabla \mathbf{U} \right) = -\nabla P + \mathbf{J} \times \mathbf{B} + \rho \mathbf{F}_g$$

The acceleration of the solar wind can be explained in terms of the conservation of mass, momentum and energy with some heating.

In steady-state

$$\nabla \cdot (\rho \mathbf{U}) = 0$$

$$\rho (\mathbf{U} \cdot \nabla \mathbf{U}) = -\nabla P + \mathbf{J} \times \mathbf{B} + \rho \mathbf{F}_g$$



Solar Wind Acceleration - 8

An analogous problem appears with the Sun case in which the flow starts subsonic and later becomes supersonic. Let us now consider this case and start with the conservation of mass and momentum (in spherical coordinates):

$$\begin{aligned}\rho(r)U(r)r^2 &= \text{constant} \\ &= \rho_0 U_0 r_0^2\end{aligned}$$

$$U \frac{dU}{dr} = - \frac{d(2n\kappa_B T)}{dr} - \rho \frac{GM_s}{r^2}$$

Using: $\rho = nM$, $P = n\kappa_B T$, $W^2 = 2\kappa_B T/M$ and $\nabla \cdot (nMU) = 0$

$$\frac{1}{U} \frac{dU}{dr} \left(\underbrace{\frac{U^2}{W^2}}_{\text{Ratio of flow speed to the thermal speed.}} - 1 \right) = \left(\underbrace{\frac{2}{r} - \frac{GM_s}{r^2 W^2} - \frac{1}{W^2} \frac{dW^2}{dr}}_{\text{This plays the role of } dA/A} \right) \quad \text{EQ-2}$$



HomeWork#1

Derive Parker hydrodynamic solution from the steady-state fluid MHD equations with the conditions indicated below and analyze the results in comparison to de Laval Nozzle solution:

$$\frac{1}{U} \frac{dU}{dr} \left(\underbrace{\frac{U^2}{W^2}}_{\substack{\text{Ratio of flow speed} \\ \text{to the thermal speed.}}} - 1 \right) = \left(\underbrace{\frac{2}{r} - \frac{GM_s}{r^2 W^2} - \frac{1}{W^2} \frac{dW^2}{dr}}_{\text{This plays the role of } dA/A} \right) \quad \text{EQ-2}$$

Conditions:

$$\frac{\partial \rho}{\partial t} + \nabla \cdot (\rho \mathbf{U}) = 0, \quad \rho \left(\frac{\partial \mathbf{U}}{\partial t} + \mathbf{U} \cdot \nabla \mathbf{U} \right) = -\nabla P + \mathbf{J} \times \mathbf{B} + \rho \mathbf{F}_g$$

$$\mathbf{U} = U(r) \mathbf{e}_r, \quad \mathbf{F}_g = -\frac{GM_s}{r^2} \mathbf{e}_r, \quad \nabla P = \frac{dP}{dr} \mathbf{e}_r, \quad \rho(r) U(r) r^2 = \text{constant} \\ = \rho_0 U_0 r_0^2$$

Using: $\rho = nM$, $P = n\kappa_B T$, $W^2 = 2\kappa_B T/M$ and $\nabla \cdot (nM\mathbf{U}) = 0$



Solar Wind Acceleration - 9

From EQ-2 Parker obtained his famous supersonic solution. Parker show that the transition from subsonic to supersonic solution occurred at the point $r = R_c$ in a constant temperature gas.

$$R_c = \frac{GM_s}{2W^2}$$

EQ-2 can be rewritten for a constant (uniform) temperature gas as:

$$U \frac{dU}{dr} \left(1 - \frac{W^2}{U^2} \right) = \frac{2W^2}{r^2} (r - R_c) \quad \text{EQ-3}$$

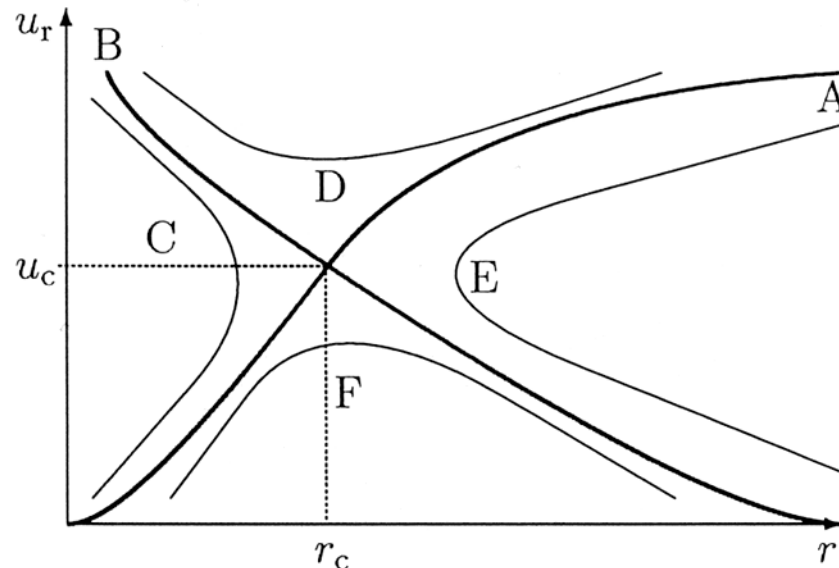


Solar Wind Acceleration - 10

This equation (EQ-3) is integrable and yields EQ-4 below:

$$\frac{U^2}{W^2} - \ln\left(\frac{U^2}{W^2}\right) = 4 \ln\left(\frac{r}{R_c}\right) + \frac{4r}{R_c} - 3 + c, \quad c = \text{integ. constant} \quad \text{EQ-4}$$

Solutions to this equation are:



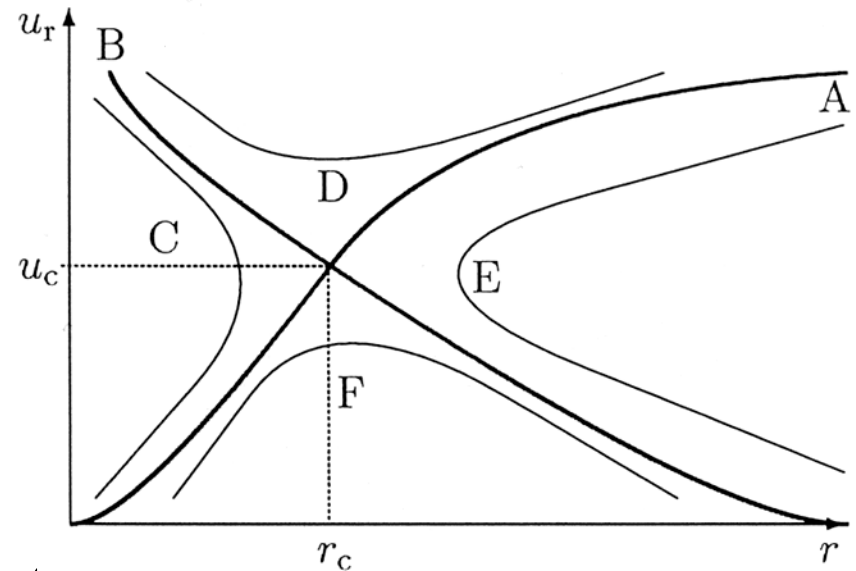


Solar Wind Acceleration -11

Solution A is the “observed” solar wind. It starts as a subsonic flow in the lower corona and accelerates with increasing radius. At the critical point the solar wind becomes supersonic.

Solution F the speed increases only weakly with height and the critical velocity is not reached. For this case the solar wind is a “solar breeze”.

Solution C the flow accelerates too fast, becomes supersonic before reaching the critical radius and turns around and flows into the Sun.

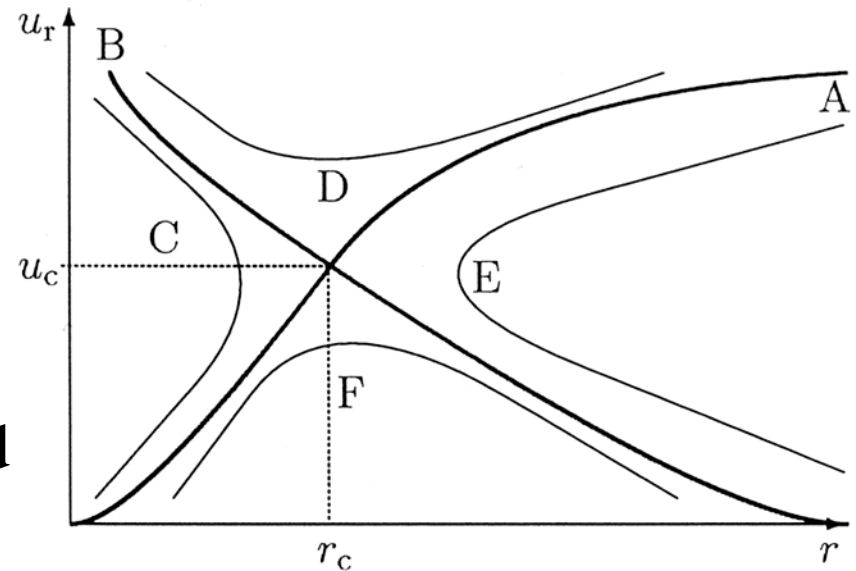




Solar Wind Acceleration -12

Solution B starts as a supersonic flow in the lower corona and becomes subsonic at the critical point. If the flow decelerates less as in D it would still be supersonic at the critical point and be accelerated again.

Solution E is an inward blowing wind that is subsonic. The flow accelerates as it approaches the Sun, turns back and leaves the Sun supersonically.

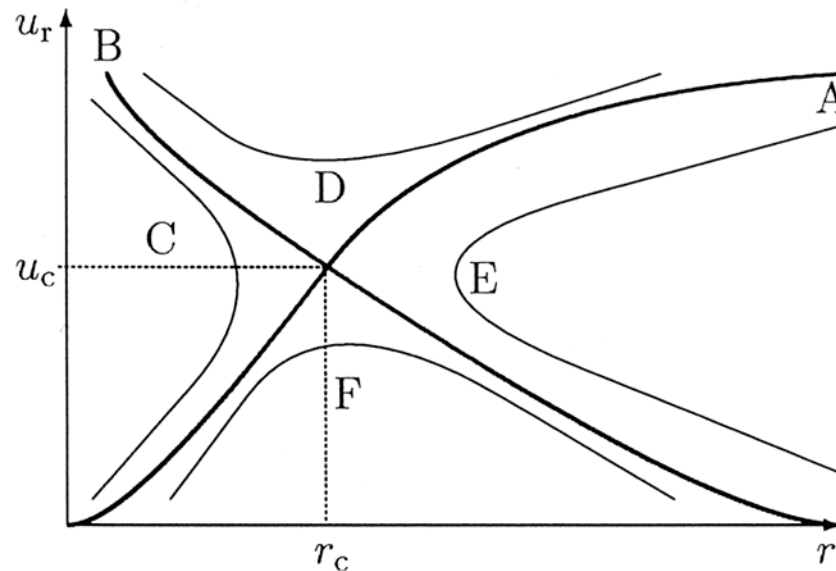




HomeWork#2

Solves numerically EQ4 and show the graphical solutions for various cases using any software you have available (e.g. IDL, Matlab, Python, Mathematica, etc). Discuss the results.

$$\frac{U^2}{W^2} - \ln\left(\frac{U^2}{W^2}\right) = 4 \ln\left(\frac{r}{R_c}\right) + \frac{4r}{R_c} - 3 + c, \quad c = \text{integ. constant} \quad \text{EQ-4}$$

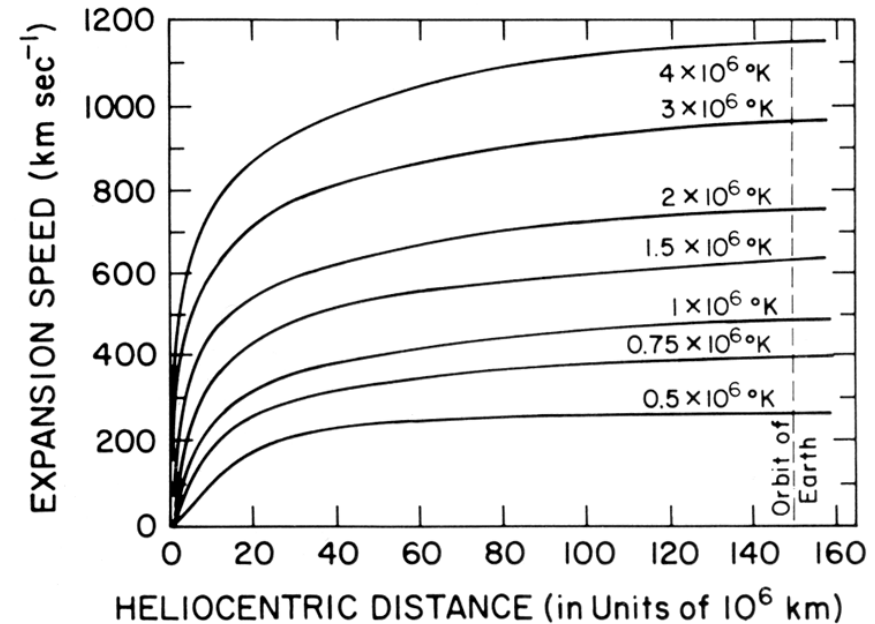




Solar Wind Acceleration -13

Following quantitative solutions (after *Parker* [1958]) it is obtained (see Figure right):

For the solar wind to continue to accelerate the mean thermal energy must exceed the gravitational energy.



To have a solar wind, a star must have a cool lower atmosphere and a hot outer atmosphere. Following similar derivation but using $\gamma = 5/3$ you can show that there is no solution that reaches supersonic speed, i.e., the solar wind does not accelerate unless there is heating. Actually only for $1 < \gamma < 5/3$ can reach supersonic speeds.



Solar Wind Heating - 1

The solar wind heating is provided by electrons:

At 10^6 degrees, electrons have thermal speeds $>1000\text{km/s}$

At 10^6 degrees, ions have thermal speeds $< 100\text{km/s}$

Electrons move along field lines faster, create an electric (ambipolar) field, pull ions

Heating of the base in the solar corona provides energy for acceleration

Using equation of energy conservation you can prove that

The initial energy in the enthalpy minus potential energy in the solar gravity

Final energy is in the kinetic energy of the solar wind

Energy transformation depletes enthalpy and increases solar wind speed to supersonic speeds



Solar Wind Heating - 2

Waves and turbulence?

One possibility is that the corona is heated by **compressional waves** at or just below the surface. Oscillatory motion of the Sun's surface could drive pressure waves. In theory fast mode waves could propagate up to $20R_{\text{Sun}}$. Experiments designed to detect sound waves propagating into the corona have not detected them.

Impulsive energy release?

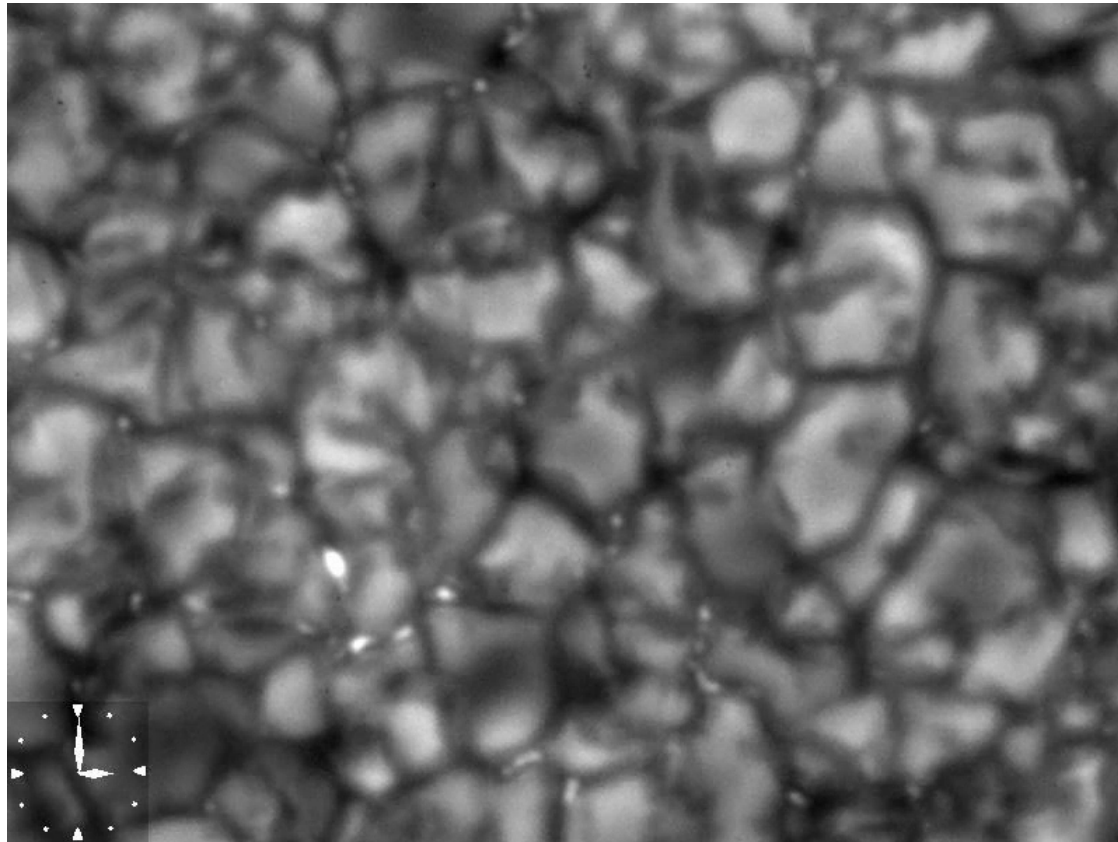
The Sun has a magnetic field that contains magnetic energy. Magnetic energy can be converted into thermal energy. This is done by **reconnection**. The granularity of the photosphere as the top of the convection zone is caused by bubbles rising and falling. These might reconnect. X-ray bursts may be evidence of this happening.

OTHER?We still don't know how the corona is heated!



Solar Wind Heating & Acceleration

- As the feet of the field lines move they are twisted and since they can't cross current sheets develop. Reconnection across these current sheets is thought to heat the corona.



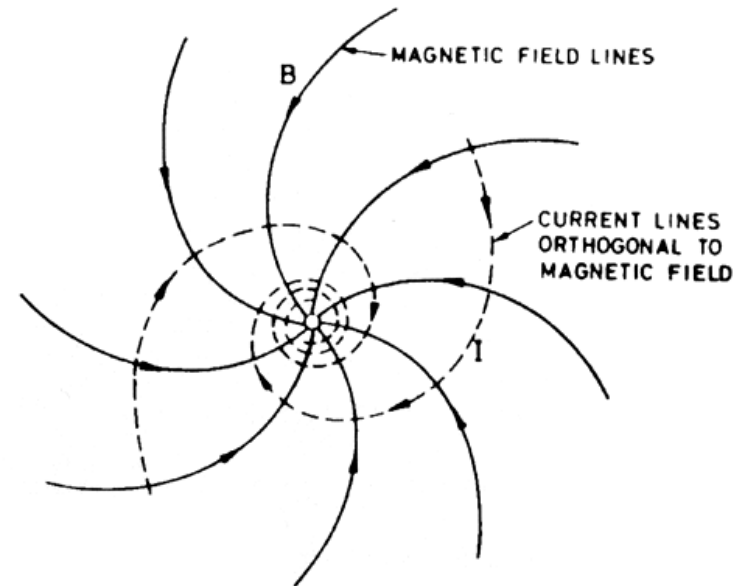
Motion of granules and
magnetic structures
– Hinode observations



Interplanetary Magnetic Field (IMF)-1

- Intermixed with the outflowing solar wind is a weak magnetic field – the interplanetary magnetic field (IMF).

- On the average the IMF is in the ecliptic plane at the orbit of the Earth although at times it can have substantial components perpendicular to the ecliptic.
- The hot coronal plasma has extremely high electrical conductivity and the IMF becomes “frozen in” to the flow.



- If the Sun did not rotate the resulting magnetic configuration would be very simple: magnetic field lines stretching approximately radially from the Sun.
- As the Sun rotates (sidereal period 27 days) the base of the field line frozen into the plasma rotates westward creating an Archimedean spiral.



Kinetics Concepts of the Solar Wind & Corona

The Kinetic plasma physics of the solar corona and solar wind system is reviewed with emphasis on the theoretical understanding of

- in situ measurements of solar wind particles and waves as measured in the solar wind
- remote-sensing observations of the solar corona made by means of ultraviolet spectroscopy and imaging provided especially by the optical instruments on SOHO



Kinetics Concepts of the Solar Wind & Corona Motivation

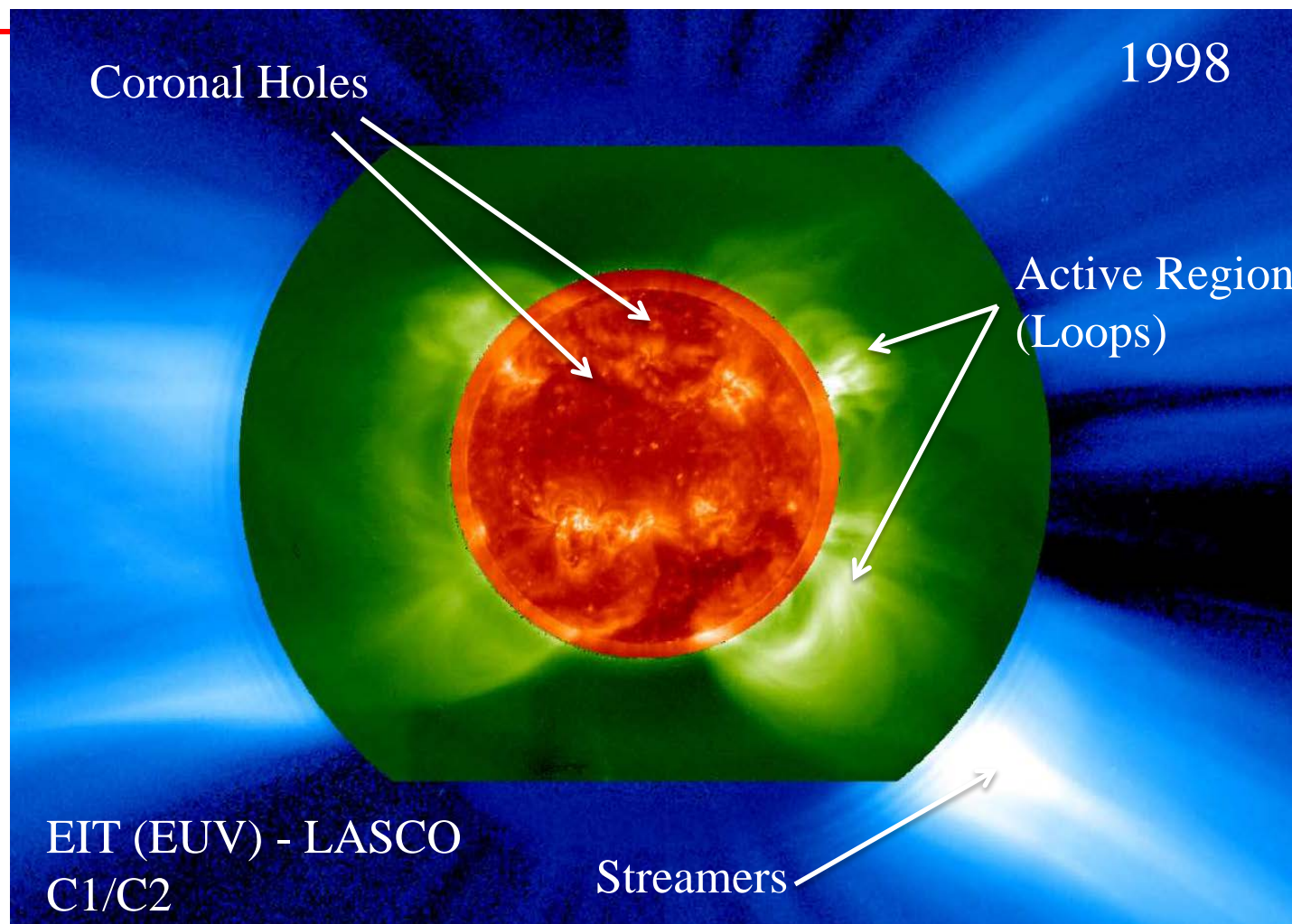
To understand coronal and solar wind heating and elucidate the microphysics of the dissipation

- Non-thermal electron and ion VDF's
- Landau- and cyclotron-resonant damping of plasma waves
- Wave absorption and microinstabilities
- Coulomb collisions in the solar wind
- Diffusion and wave-particle interactions
- Virtues and limitations of fluid models (single/multi-species) or magnetohydrodynamic, multi-moment models and Kinetic models for coronal heating and solar wind acceleration



Kinetics Concepts of the Solar Wind & Corona

Corona of the Active Sun



The solar corona as seen by 3 instruments onboard SOHO (EIT at the center, and LASCO C1 and C2). The EIT image shows the corona in EUV light, with the bright regions representing the active regions on the Sun (loop-like structures), and the darker polar regions representing coronal holes.



Kinetics Concepts of the Solar Wind & Corona

Solar Sources and Types of the Solar Wind

- **High Speed Wind**

- **Low Density**

- **Low Variability**

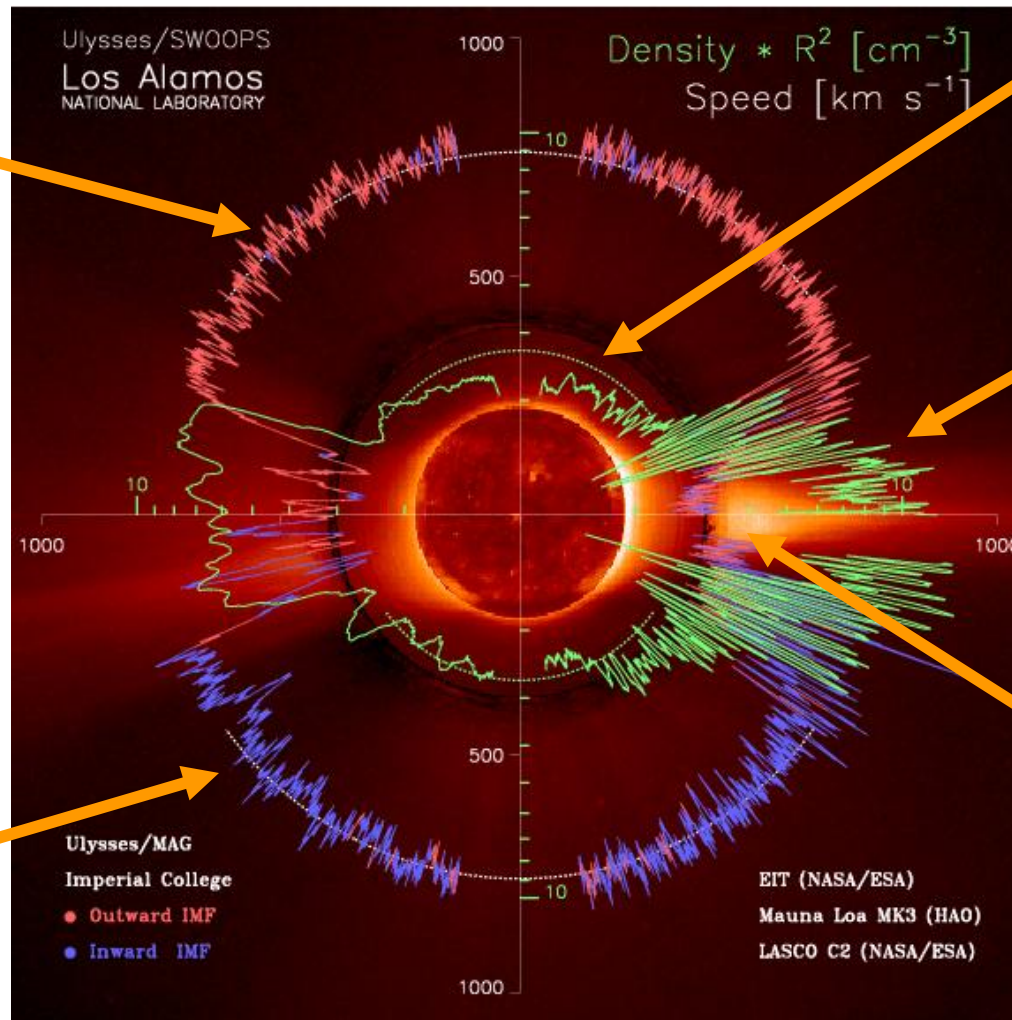
- **Positive Polarity**

- **High Speed Wind**

- **Low Density**

- **Low Variability**

- **Negative Polarity**



- **Polar Coronal Hole**

- **Slow Wind**

- **High Density**

- **Variable**

- **Mixed Polarity**

- **Streamers**

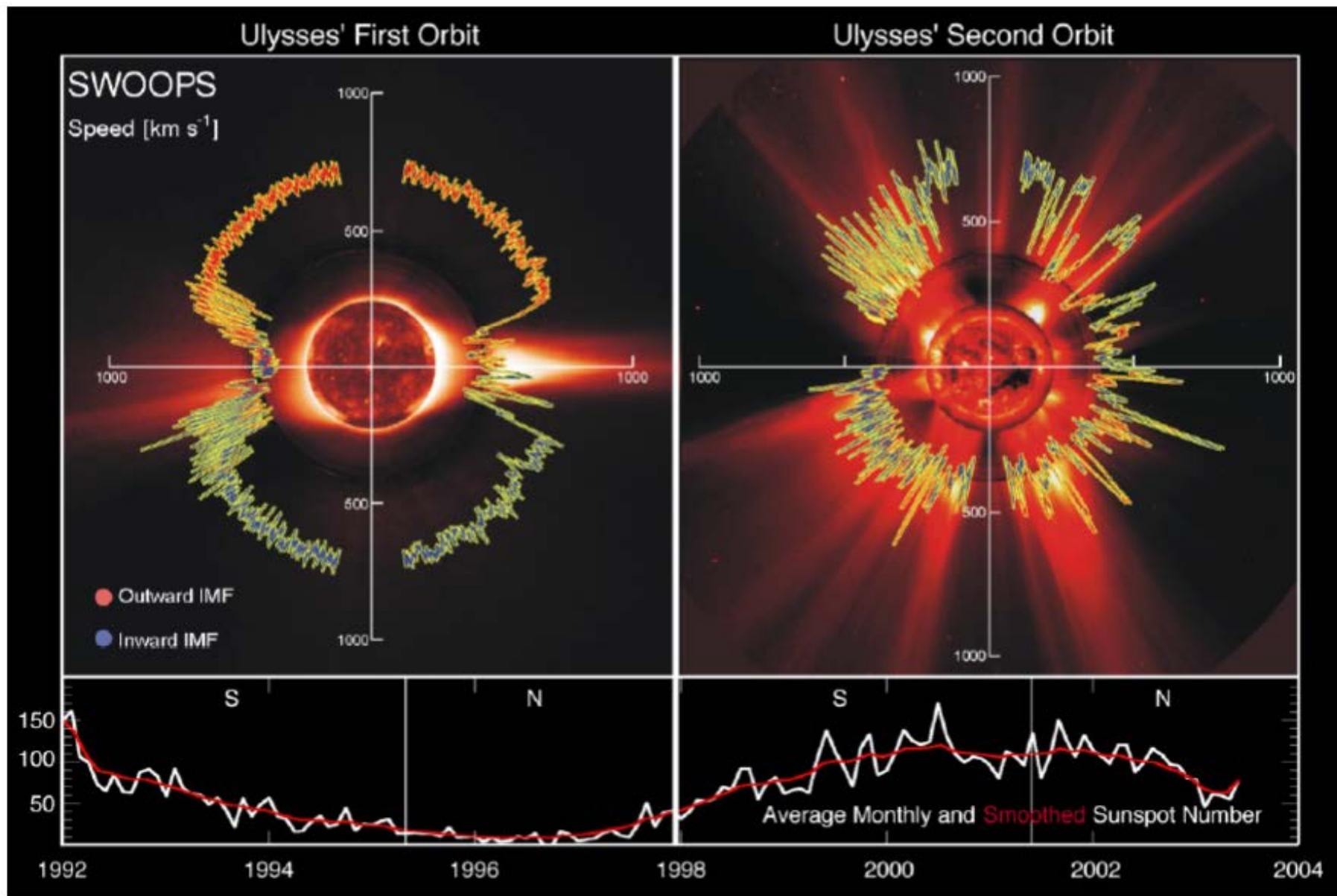
McComas et al., JGR, 105,10419, 2000.

Ulysses/SWOOPS speed, density and EIT/LASCO/Mauna Loa images.



Kinetics Concepts of the Solar Wind & Corona

Min & Max Coronal Structures



Coronal & SW heating problem what does it mean?

Mechanical and magnetic energy:

- Generation/release
- Transport/propagation
- Conversion/dissipation
 - Magnetoconvection, restructuring of fields and magnetic reconnection
 - Non-thermal distributions
 - Magnetohydrodynamic + plasma waves, shocks
 - Ohmic + microturbulent heating, radiative cooling, resonance absorption



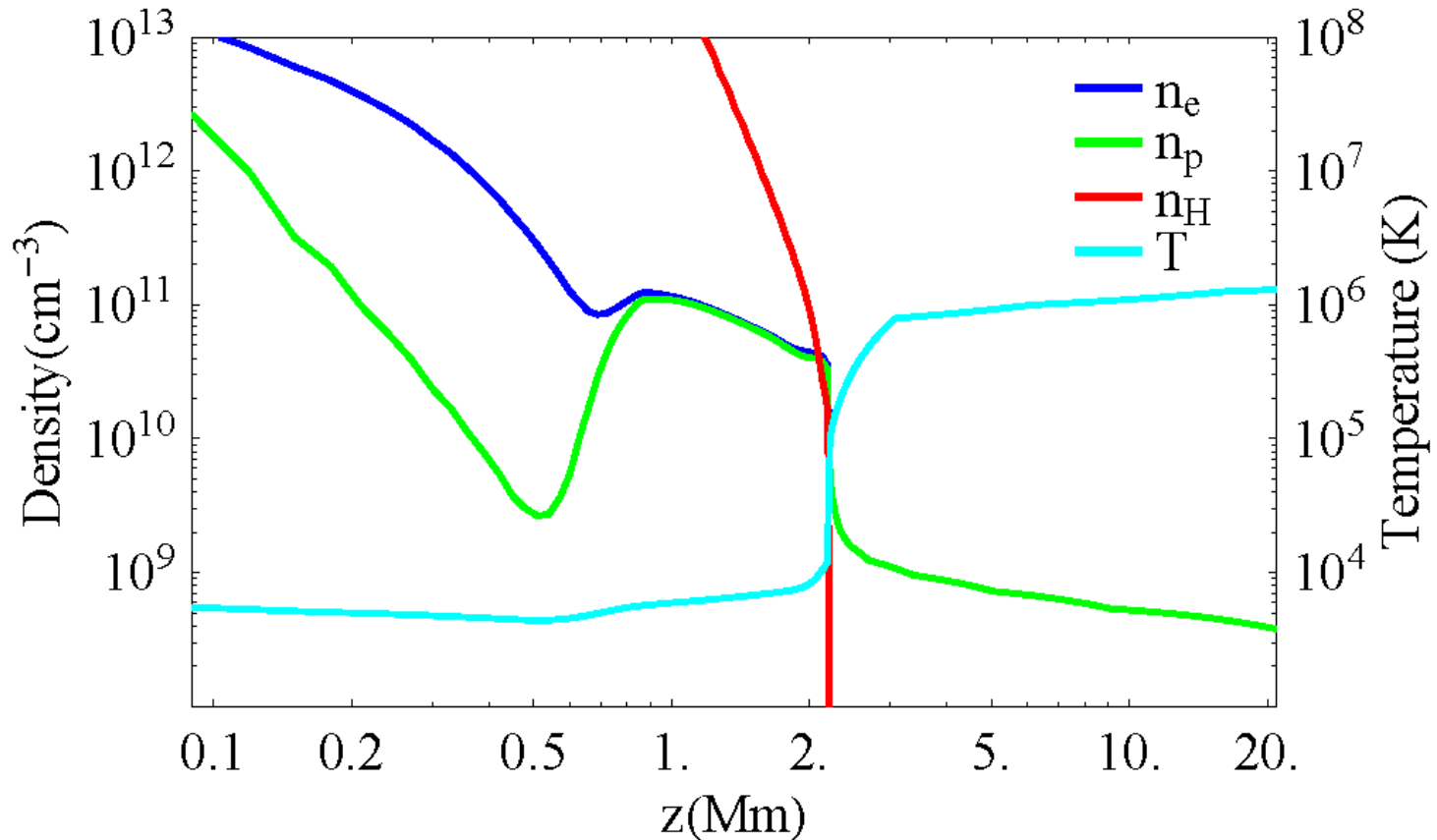
Kinetic processes in the solar corona and solar wind

- Plasma is multi-component and nonuniform
 - **complexity**
- Plasma is dilute
 - **deviations from local thermal equilibrium**
 - **suprathermal particles (electron strahl)**
 - **global boundaries are reflected locally**

Problem: Thermodynamics of the plasma, which is far from equilibrium..... **Non-LTE**



Density & Temperature Profiles



Electron density n_e , proton density n_p , neutral hydrogen density n_H and the temperature T as a function of height z in the solar atmosphere, as obtained from the chromospheric model (FAL-C) of Fontenla et al. (1993) and the model for the lower corona of Gabriel (1976)



Collision Frequencies & Mean Free Paths

1 AU ~ 1.496 x 10⁸ km

Parameter	Chromo- sphere	Corona (1.3R _S)	Solar wind (1AU)
n _e /cm ⁻³	10 ¹⁰	10 ⁷	10
T _e /K	10 ³	1-2 10 ⁶	10 ⁵
λ /km	≤1	10 ³	10 ⁷

$$\lambda_{mf} = v_{th,e} / \nu_{ei}, \quad n_e \approx \sum_i Z_i n_i$$

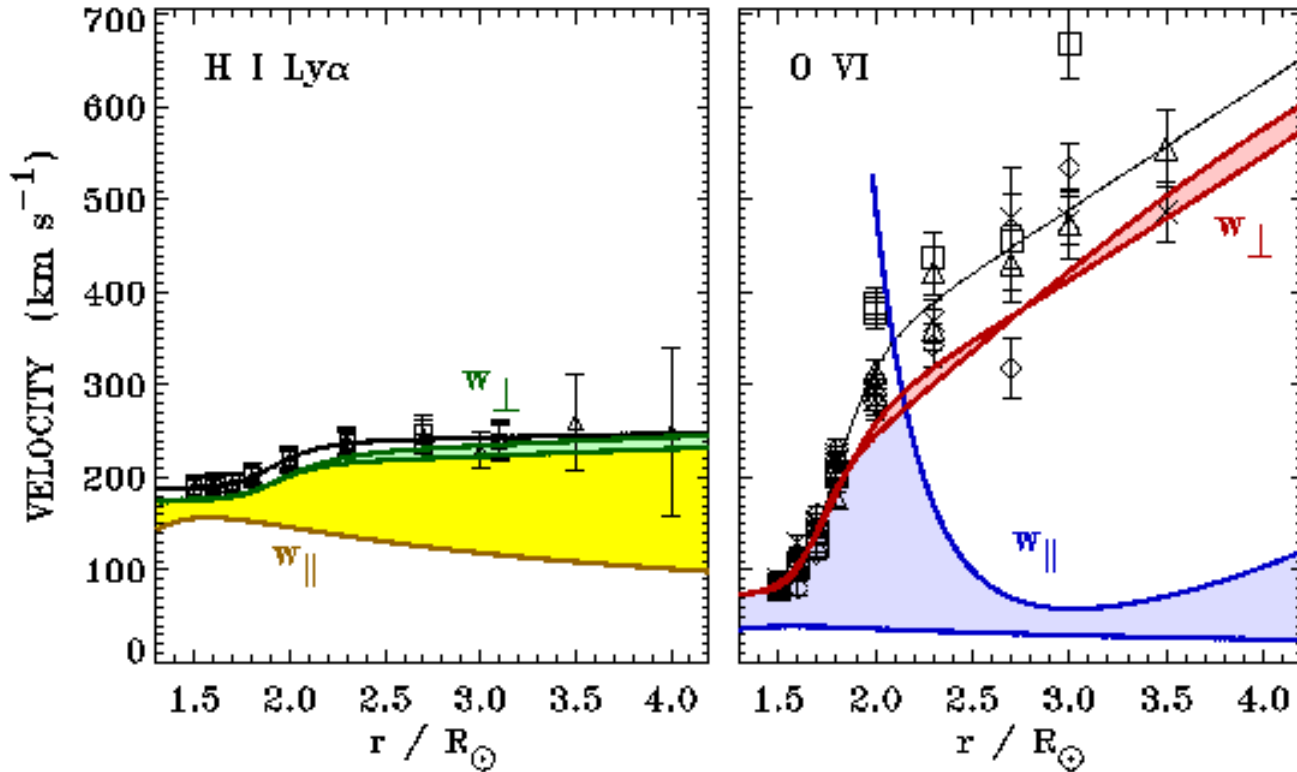
$$\nu_{ei} = \frac{4\sqrt{2\pi} n_i Z_i^2 e^4 \ln \Lambda}{3m_e^{1/2} T_e^{3/2}}$$

$$\nu_{ii} = \frac{4\sqrt{2\pi} n_i Z_i^2 e^4 \ln \Lambda}{3m_i^{1/2} T_i^{3/2}}$$

$$\nu_{ee} \sim \nu_{ei} \gg \nu_{ii}, \nu_{ie}$$



Oxygen and hydrogen thermal speeds in coronal holes



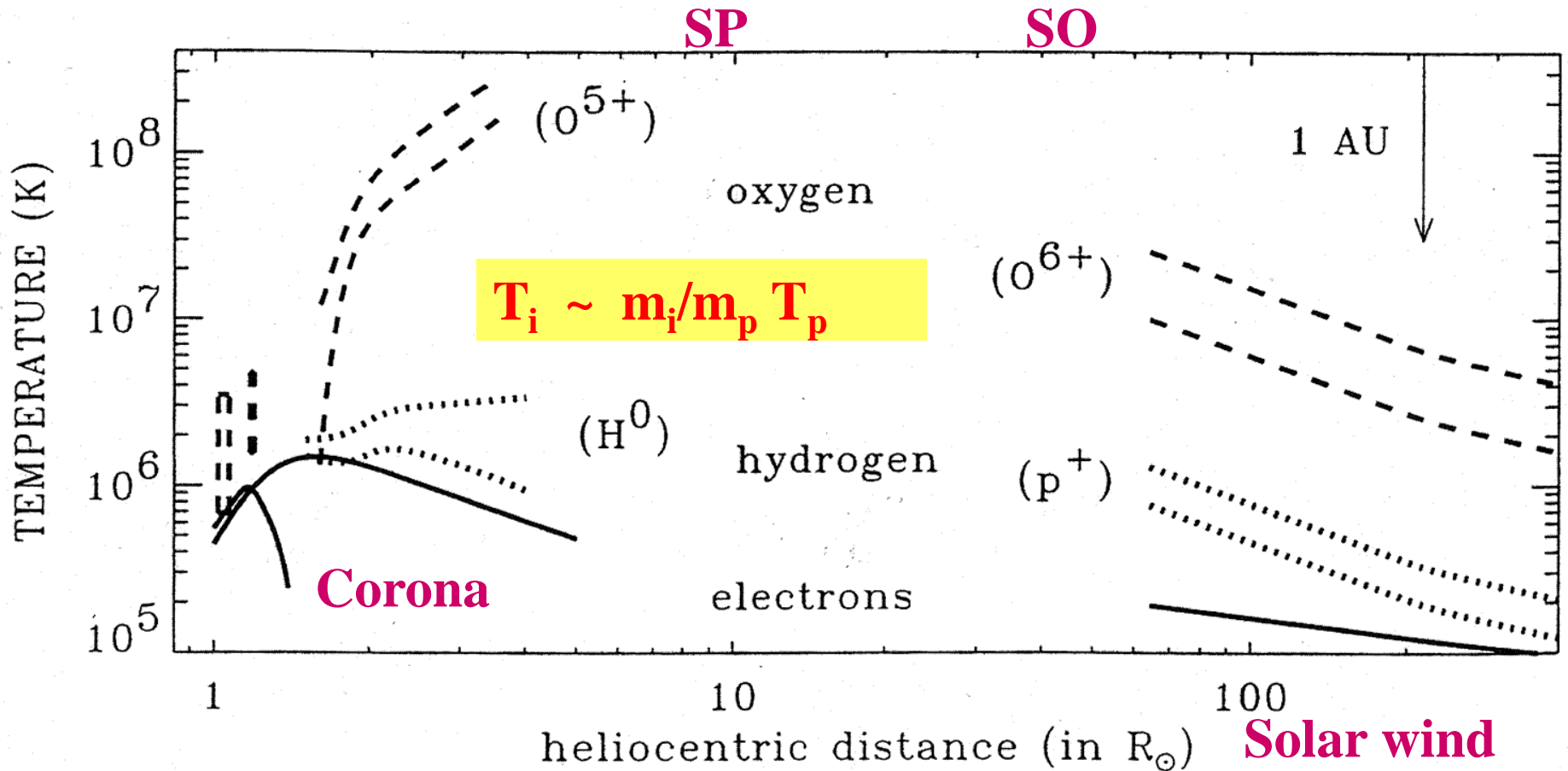
Very Strong
perpendicular
heating of
Oxygen !

Cranmer et al., Ap. J.,
511, 481, 1998

Large anisotropy: $T_{O\perp}/T_{O\parallel} \geq 10$



Temperature profiles in the corona and fast solar wind





Length Scales in the Solar Wind

Macrostructure - fluid scales

- Heliocentric distance: r 150 Gm (1AU)
- Solar radius: R_s 696000 km (215 R_s)
- Coronal Loops L 100 – 400 Mm
- Alfvén waves: λ 30 - 100 Mm

Microstructure - kinetic scales

- Coulomb free path: λ_{mfp} ~ 0.1 - 10 AU
- Ion inertial length: V_A/Ω_p (c/ω_p) ~ 100 km
- Ion gyroradius: r_L ~ 50 km
- Debye length: λ_D ~ 10 m
- Helios/Wind spacecraft: d ~ 3 m

Microscales vary with solar distance!

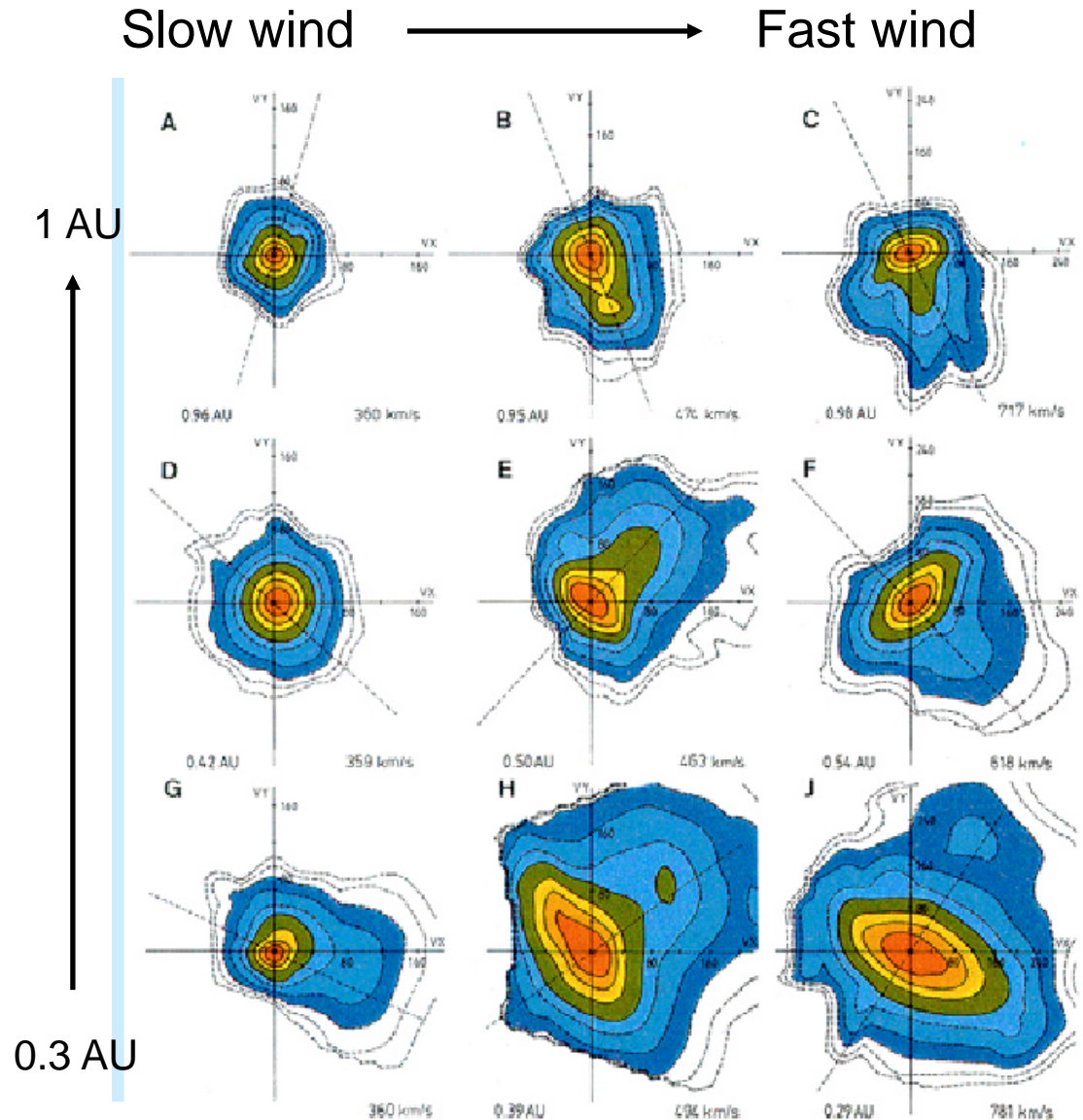


Solar Wind Ions: Non-Thermal Distributions

Proton solar wind
distribution functions
Marsch et al., JGR, 87,
52, 1982 (Helios data)

Free Energy Sources

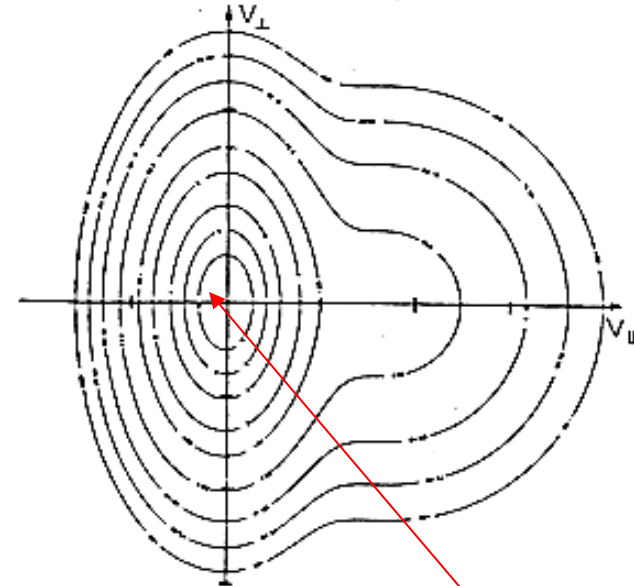
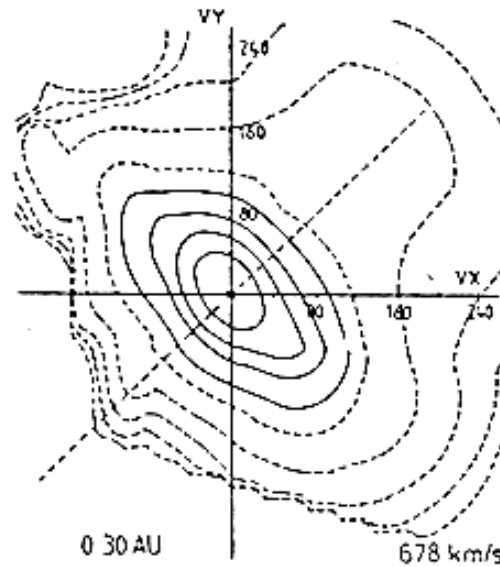
- $T_{\perp}/T_{\parallel} \neq 1$
- Nonthermal tails
- Ion Beams





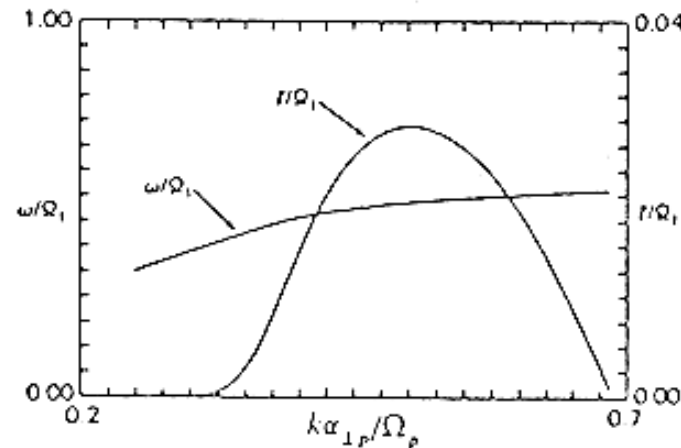
Proton Temperature Anisotropy

- Measured and modelled proton velocity distribution
- Growth of ion-cyclotron waves!
- Anisotropy-driven instability by large perpendicular T_{\perp}



anisotropy

$\omega \approx 0.5\Omega_p$
 $\gamma \approx 0.05\Omega_p$

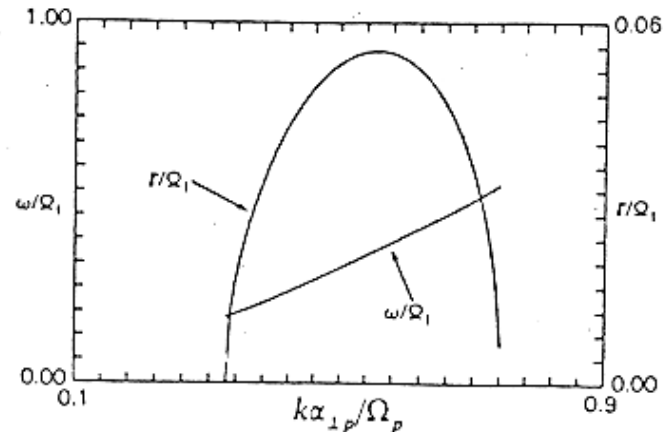
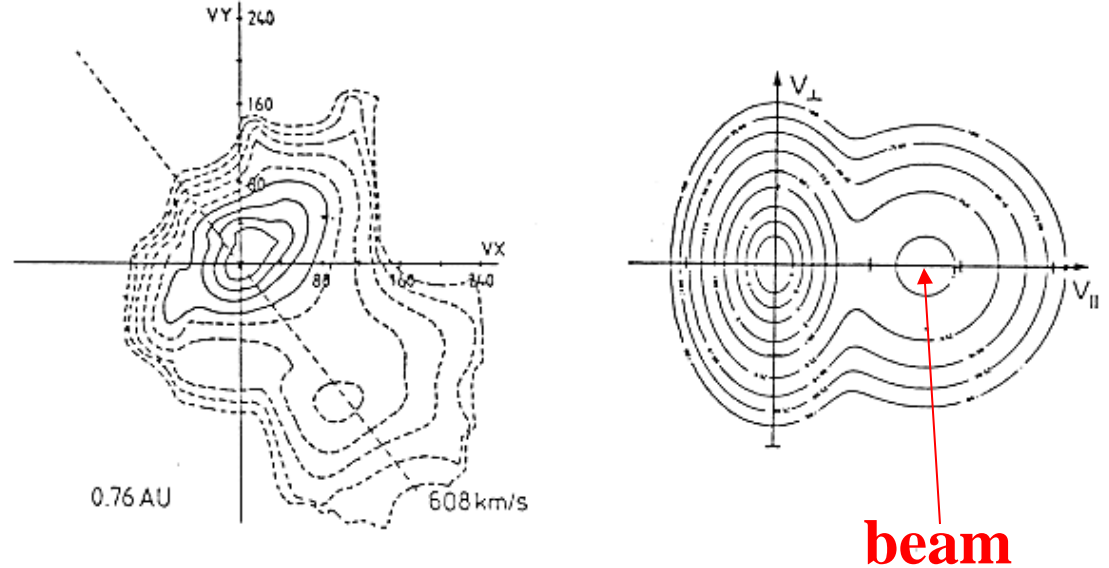




Wave Regulation of Proton Beam

- Measured and modelled velocity distribution
- Growth of fast mode waves!
- Beam-driven instability, large drift speed

$\omega \approx 0.4\Omega_p$
 $\gamma \approx 0.06\Omega_p$





Electron energy spectrum

IMP
spacecraft

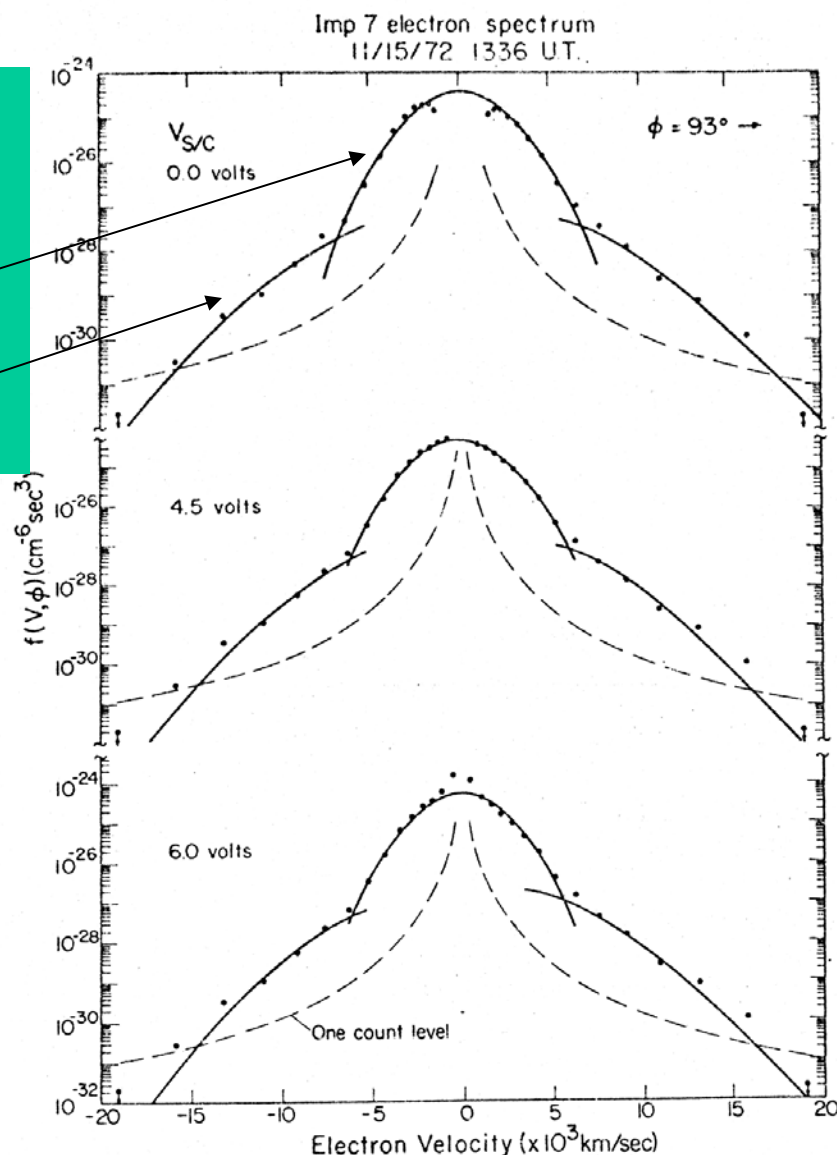
Two solar wind
electron populations:

- Core (96%)
- Halo (4%)

Core: local, collisional, **bound**
by **electrostatic potential**

Halo: global, collisionless,
free to escape (exospheric)

Feldman et al., JGR, **80**,
4181, 1975

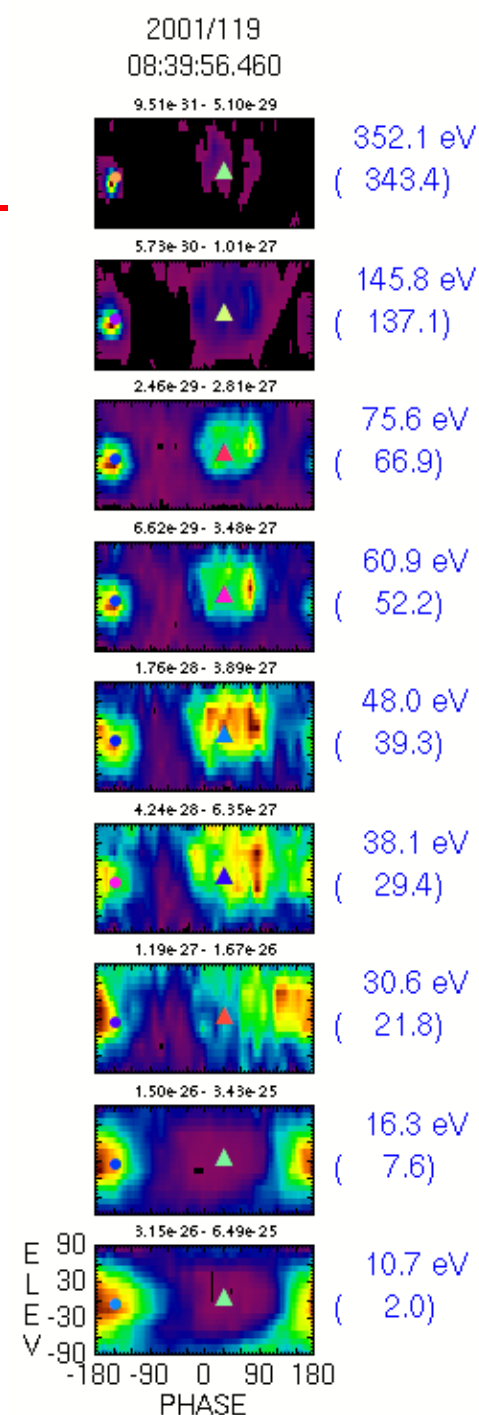




Electron Components Quick Overview

The solar wind electron VDF generally consists of three main populations:

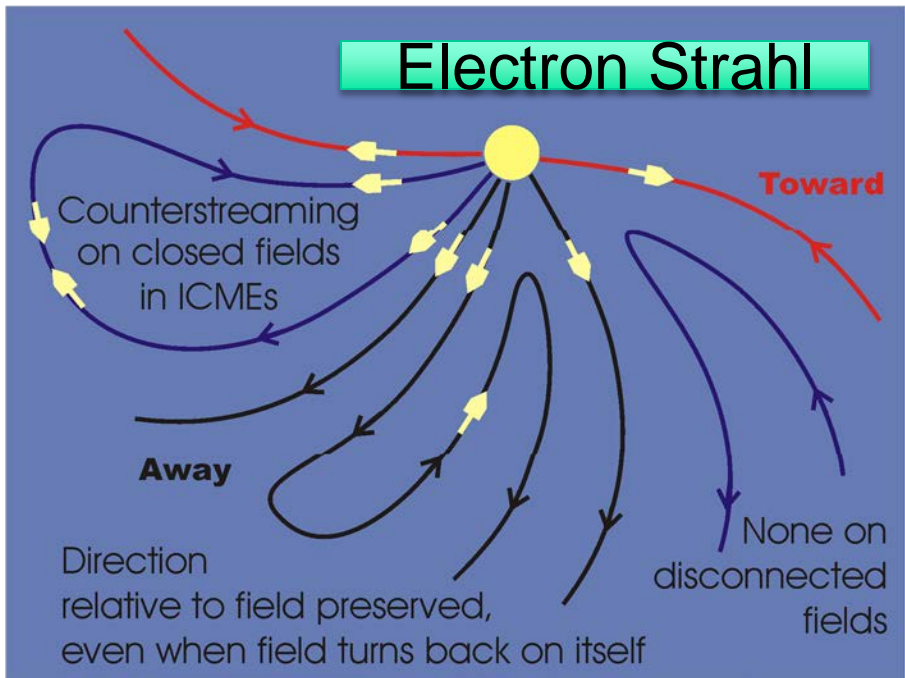
- **Core Electrons** (below 10-15eV, 95%, thermal isotropic Maxwellian)
- **Halo Electrons** (above 15 to 100eV, 4%, non-thermal, slightly anisotropic, Lorentzian/Tsallis kappa-like VDF) (observed at all pitch-angles)
- **Strahl Electrons** (0.05-1 keV, non-thermal, field-aligned, confined to a solid-angle cone < 90 deg.)





Strahl Flow Velocity and Magnetic Field Correlation

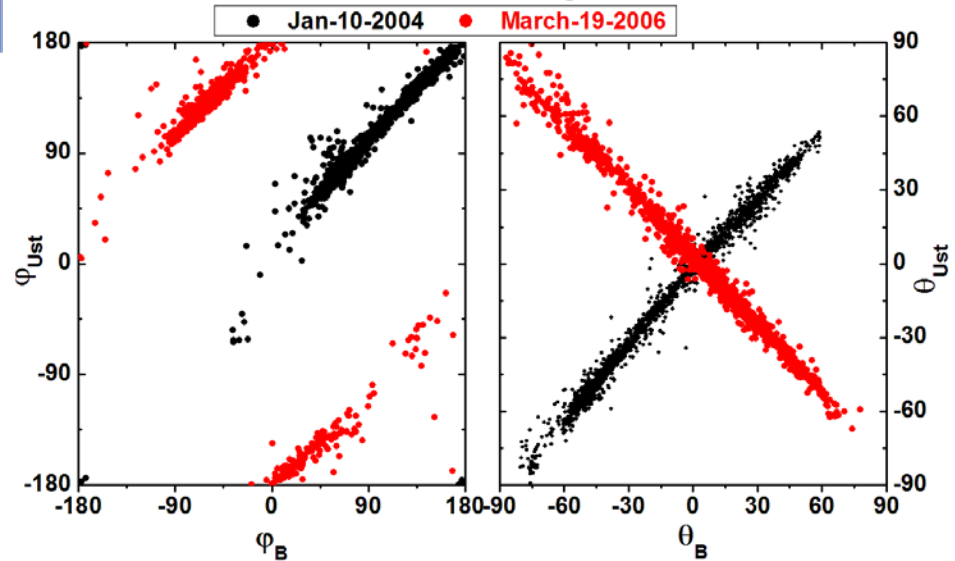
Electron Strahl



Cluster Strahl Moment Bulk Velocity
Generated by the SPH spectral Model
(Viñas & Gurgiolo, JGR/2009)



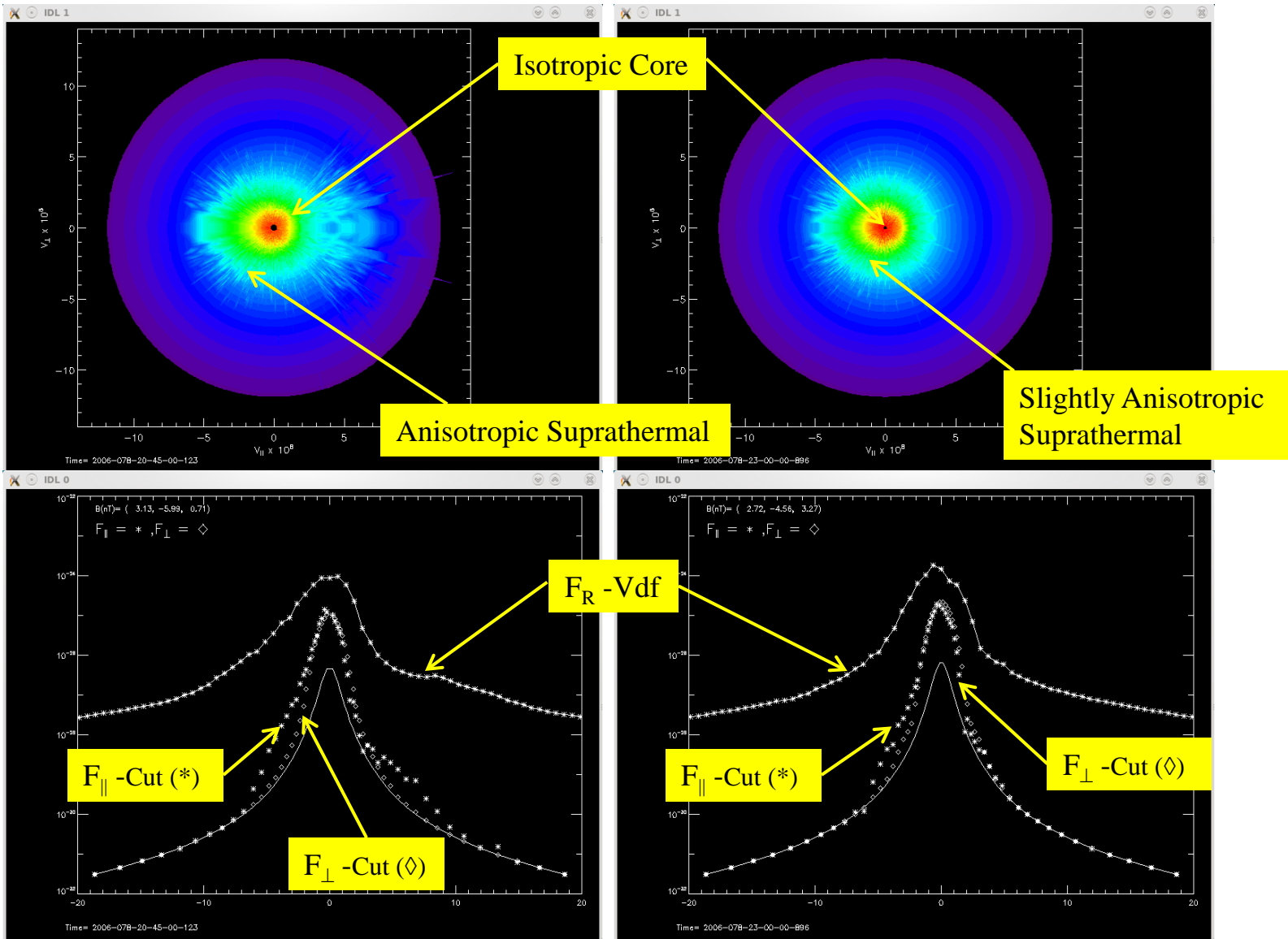
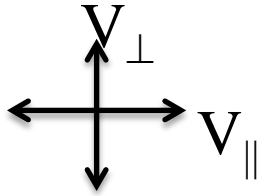
Correlation of the Strahl Flow Velocity and Magnetic Field
Azimuthal and Polar Angles





Cluster Velocity Distribution Functions

$$f_e(v_{\parallel}, v_{\perp})$$

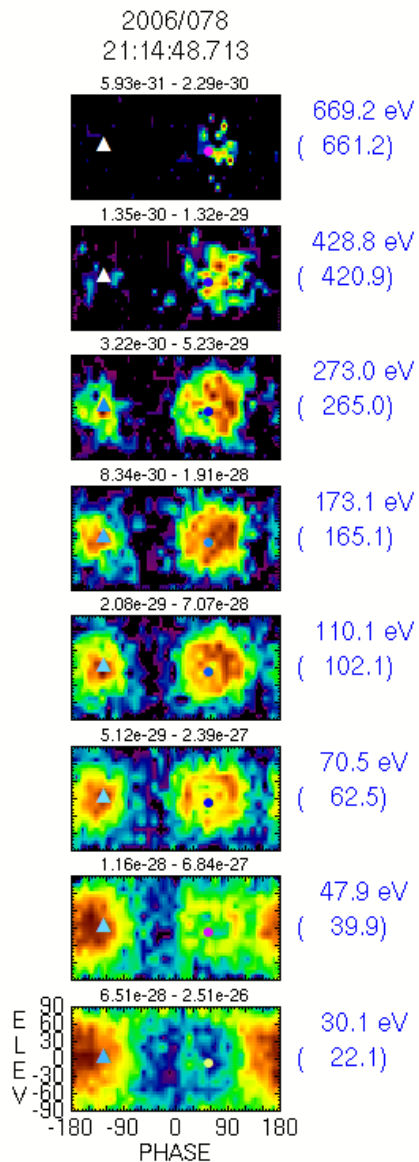




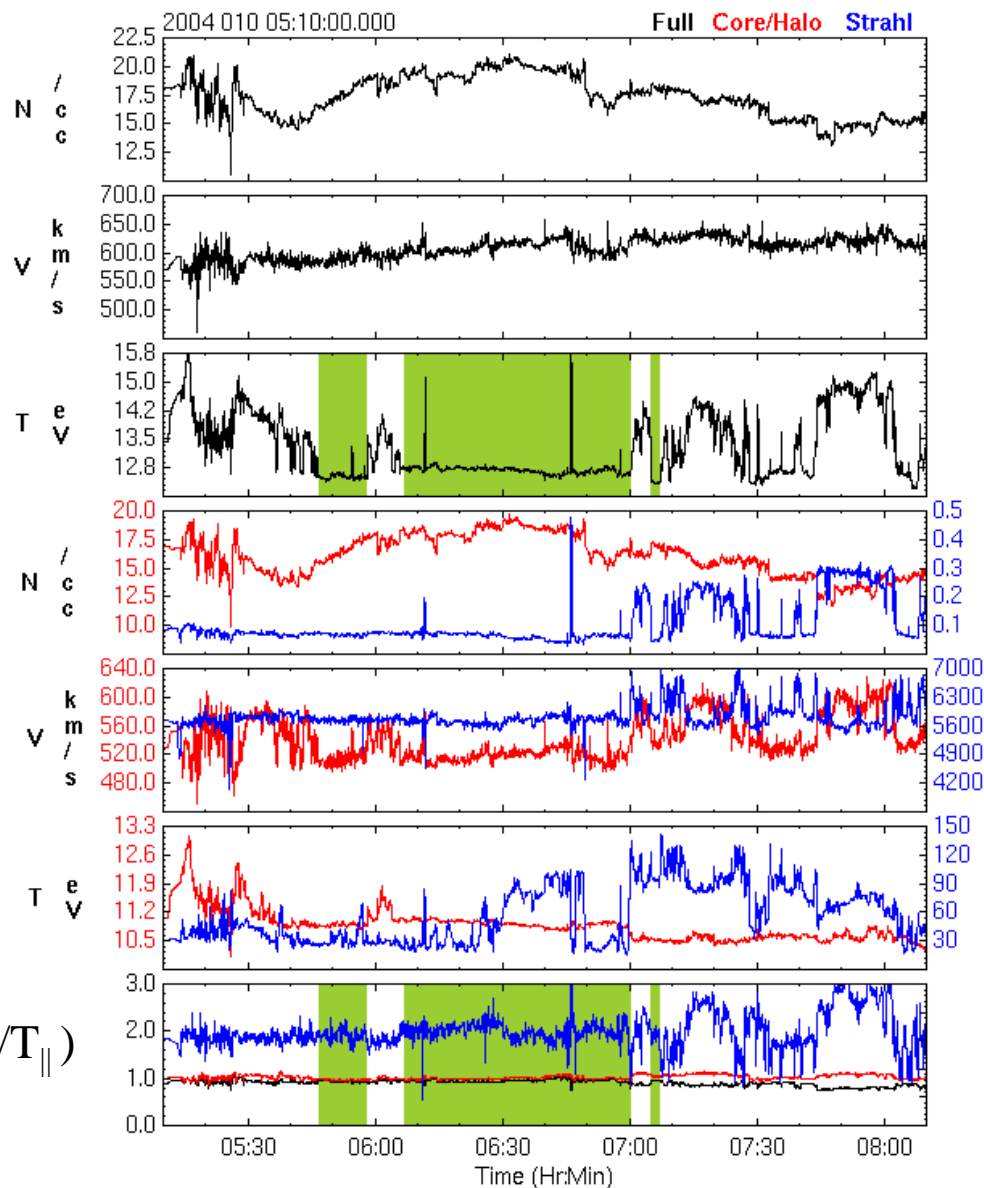
Cluster-2 Electron Moments

Event: 2004-010
05:10-08:15

CLUSTER-2 Electron Moments and MF



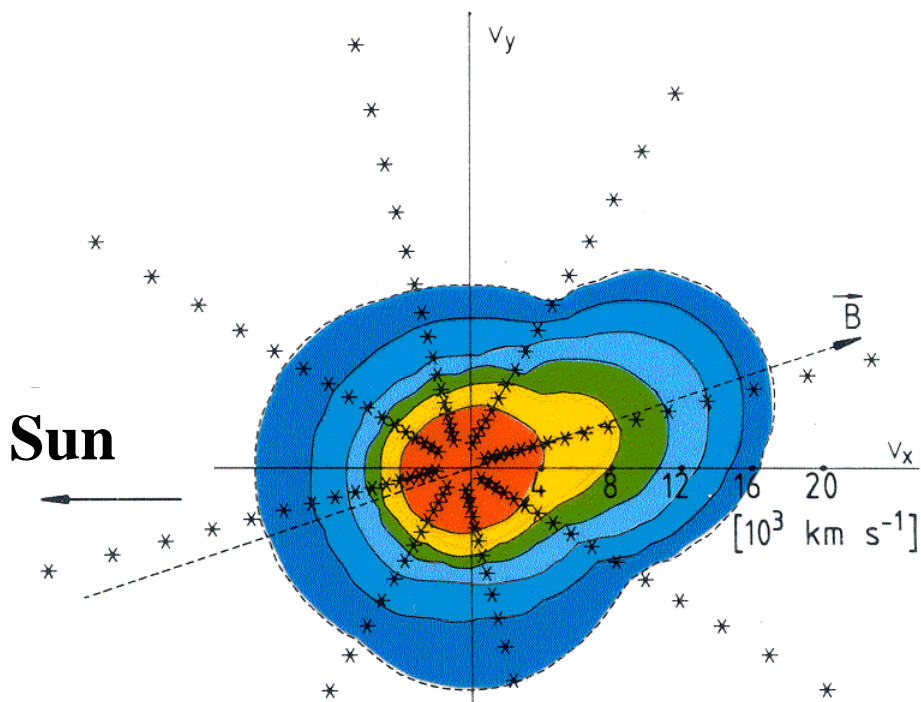
$$(T_{\perp}/T_{\parallel})$$





Electron velocity distribution function

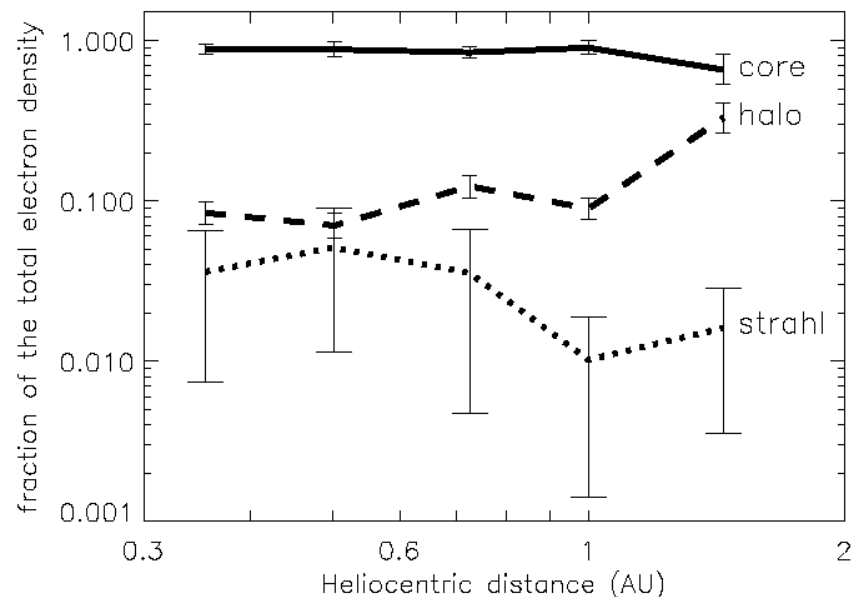
Helios



$n_e = 3-10 \text{ cm}^{-3}$

Pilipp et al., JGR,
92, 1075, 1987

- **Non-Maxwellian**
- **Heat flux tail**



Radial decline (increase) of the number of strahl (halo) electrons with heliocentric distance from the Sun according to the Helios, WIND and Ulysses measurements (after Maksimovic et al., 2005).



Kinetic plasma instabilities

- Observed velocity distributions at the margin of stability
- Selfconsistent quasi- or non-linear effects not well understood
- Wave-particle interactions are the key to understand ion kinetics in corona and solar wind!

Wave mode	Free energy source
Ion acoustic	Ion beams, electron heat flux
Ion cyclotron	Temperature anisotropy
Whistler (Lower Hybrid)	Electron heat flux
Magnetosonic	Ion beams, differential streaming

Marsch, 1991; Gary, Space Science Rev., **56**, 373, 1991



Theoretical description

Boltzmann-Vlasov kinetic equations for protons, alpha-particles (4%), minor ions and electrons

Distribution functions

Kinetic equations

- + Coulomb collisions (Landau)
 - + Wave-particle interactions
 - + Micro-instabilities (Quasilinear)
 - + Boundary conditions
- **Particle velocity distributions and field power spectra**

Moments

Multi-Fluid (MHD) equations

- + Collision terms
 - + Wave (bulk) forces
 - + Energy addition
 - + Boundary conditions
- **Single/multi fluid parameters**



Velocity distribution functions

Statistical description: $f_j(\mathbf{x}, \mathbf{v}, t) d^3x d^3v$,

gives the probability to find a particle of species j with a velocity \mathbf{v} at location \mathbf{x} at time t in the 6-dimensional phase space.

Local thermodynamic equilibrium:

$$f_j^M(\mathbf{x}, \mathbf{v}, t) = n_j (2\pi v_j)^{-3/2} \exp[-(\mathbf{v} - \mathbf{U}_j)^2 / v_j^2],$$

with number density, n_j , thermal speed, v_j , and bulk velocity, \mathbf{U}_j , of species j .

Dynamics in phase space: Vlasov/Boltzmann kinetic equation



Fluid description

Moments of the Vlasov/Boltzmann equation:

Density: $n_j = \int d^3v f_j(\mathbf{x}, \mathbf{v}, t)$

Flow velocity: $\mathbf{U}_j = 1/n_j \int d^3v f_j(\mathbf{x}, \mathbf{v}, t) \mathbf{v}$

Thermal speed: $v_j^2 = 1/(3n_j) \int d^3v f_j(\mathbf{x}, \mathbf{v}, t) (\mathbf{v}-\mathbf{U}_j)^2$

Temperature: $T_j = m_j v_j^2 / k_B$

Heat flux: $Q_j = 1/2 m_j \int d^3v f_j(\mathbf{x}, \mathbf{v}, t) (\mathbf{v}-\mathbf{U}_j) (\mathbf{v}-\mathbf{U}_j)^2$



Single MHD Description

$$\frac{\partial \rho}{\partial t} + \nabla \cdot (\rho \vec{\mathbf{U}}) = 0$$

$$\begin{aligned} \frac{\partial (\rho \vec{\mathbf{U}})}{\partial t} + \nabla \cdot \left[\rho \vec{\mathbf{U}} \vec{\mathbf{U}} - \frac{1}{4\pi} \vec{\mathbf{B}} \vec{\mathbf{B}} + \left(P + \frac{B^2}{8\pi} \right) \mathbf{I} \right] \\ + \rho \left[\frac{GM_{\odot}}{r^2} \hat{\mathbf{e}}_r + 2\Omega_{\odot} \times \vec{\mathbf{U}} + \Omega_{\odot} \times (\Omega_{\odot} \times \vec{\mathbf{r}}) \right] = \bar{\lambda}_v \nabla^2 \vec{\mathbf{U}} \end{aligned}$$

$$\frac{\partial \vec{\mathbf{B}}}{\partial t} = \nabla \times (\vec{\mathbf{U}} \times \vec{\mathbf{B}}) + \bar{\eta}_v \mathbf{J} \quad \mathbf{J} = \frac{1}{4\pi} \nabla \times \vec{\mathbf{B}} \quad \nabla \cdot \vec{\mathbf{B}} = 0$$

$$\frac{\partial P}{\partial t} + (\vec{\mathbf{U}} \cdot \nabla) P + \gamma P \nabla \cdot \vec{\mathbf{U}} + (\gamma - 1) \nabla \cdot \vec{\mathbf{q}} = \bar{Q} \quad \vec{\mathbf{q}} = -\bar{\kappa}_v \vec{\nabla} T$$



Multiple Fluid Description

$$\frac{\partial m_s n_s}{\partial t} + \nabla \cdot (m_s n_s \vec{U}_s) = 0$$

$$m_s n_s \left[\frac{\partial \vec{U}_s}{\partial t} + (\vec{U}_s \cdot \vec{\nabla}) \vec{U}_s \right] = q_s n_s \left(\vec{E} + \frac{1}{c} \vec{U}_s \times \vec{B} \right) - \vec{\nabla} P_s + m_s n_s \vec{g}_{eff} - \sum_{i(i \neq s)} m_s n_s v_{is} (\vec{U}_i - \vec{U}_s)$$

$$\vec{E} = -\frac{1}{c} (\vec{U}_e \times \vec{B}) - \frac{1}{en_e} \vec{\nabla} P_e + \frac{m_e}{e} \vec{g}_{eff} + \frac{m_e}{e} \sum_i v_{ei} (\vec{U}_e - \vec{U}_i)$$

$$-\frac{m_e}{e} \left[\frac{\partial \vec{U}_e}{\partial t} + \vec{U}_e \cdot \vec{\nabla} \vec{U}_e \right]$$

$\xrightarrow{\quad} = 0$ $\xrightarrow{\quad} = 0$

$$\frac{\partial \vec{B}}{\partial t} = \nabla \times (\vec{U} \times \vec{B}) + \bar{\eta}_v \mathbf{J}, \quad \mathbf{J} = \frac{c}{4\pi} \nabla \times \vec{B} = \sum_{s(s \neq e)} q_s n_s \vec{U}_s - en_e \vec{U}_e, \quad \nabla \cdot \vec{B} = 0$$

$$\frac{\partial P_s}{\partial t} + (\vec{U}_s \cdot \vec{\nabla}) P_s + \gamma_s P_s \nabla \cdot \vec{U}_s + (\gamma_s - 1) \nabla \cdot \vec{q}_s = \bar{Q}_s$$



Vlasov-Boltzmann/Fokker-Planck Description

$$\frac{\partial f_s}{\partial t} + \mathbf{v}_{\parallel} \nabla_s f_s + \left(\mathbf{g}_{\parallel} + \frac{q_s}{m_s} E_{\parallel} \right) \frac{\partial f_s}{\partial v_{\parallel}} + \frac{v_{\perp}}{2B} \nabla_s B \left[v_{\parallel} \frac{\partial f_s}{\partial v_{\perp}} - v_{\perp} \frac{\partial f_s}{\partial v_{\parallel}} \right] = \left(\frac{\delta f_s}{\delta t} \right)_{CC} + \left(\frac{\delta f_s}{\delta t} \right)_{WP}$$

$$\left(\frac{\delta f_s}{\delta t} \right)_{CC} = -\nabla_{\mathbf{v}} \cdot \mathbf{S}_s$$

$$\mathbf{S}_s = \sum_{s'} \mathbf{S}_{s,s'} = \sum_{s'} \frac{2\pi q_s^2 q_{s'}^2}{m_s} \ln \Lambda_{s,s'} \int \mathbf{U}(\mathbf{v} - \mathbf{v}') \cdot \left(\frac{f_s(\mathbf{v})}{m_{s'}} \frac{\partial f_{s'}(\mathbf{v}')}{\partial \mathbf{v}'} - \frac{f_{s'}(\mathbf{v}')}{m_s} \frac{\partial f_s(\mathbf{v})}{\partial \mathbf{v}} \right) d^3 \mathbf{v}'$$

$$\mathbf{S}_{s,s'} = -\mathbf{D}_{s,s'} \cdot \nabla_{\mathbf{v}} f_s + \mathbf{F}_{s,s'} f_s$$

$$\mathbf{D}_{s,s'} = -\frac{4\pi \Gamma_{s,s'}}{n_{s'}} \nabla_{\mathbf{v}} \nabla_{\mathbf{v}} \psi_{s'}(\mathbf{v}) \quad \text{and} \quad \mathbf{F}_{s,s'} = -\frac{4\pi \Gamma_{s,s'}}{n_{s'}} \frac{m_s}{m_{s'}} \nabla_{\mathbf{v}} \phi_{s'}(\mathbf{v})$$

$$\left(\frac{\delta f_s}{\delta t} \right)_{WP} = \frac{\partial}{\partial \mathbf{v}} \cdot \left(\mathbf{D} \cdot \frac{\partial f_s}{\partial \mathbf{v}} \right) = \frac{1}{v_{\perp}} \frac{\partial}{\partial v_{\perp}} \left[v_{\perp} \left(D_{\perp\perp} \frac{\partial}{\partial v_{\perp}} + D_{\perp\parallel} \frac{\partial}{\partial v_{\parallel}} \right) f_s \right] + \frac{\partial}{\partial v_{\parallel}} \left[\left(D_{\parallel\perp} \frac{\partial}{\partial v_{\perp}} + D_{\parallel\parallel} \frac{\partial}{\partial v_{\parallel}} \right) f_s \right]$$

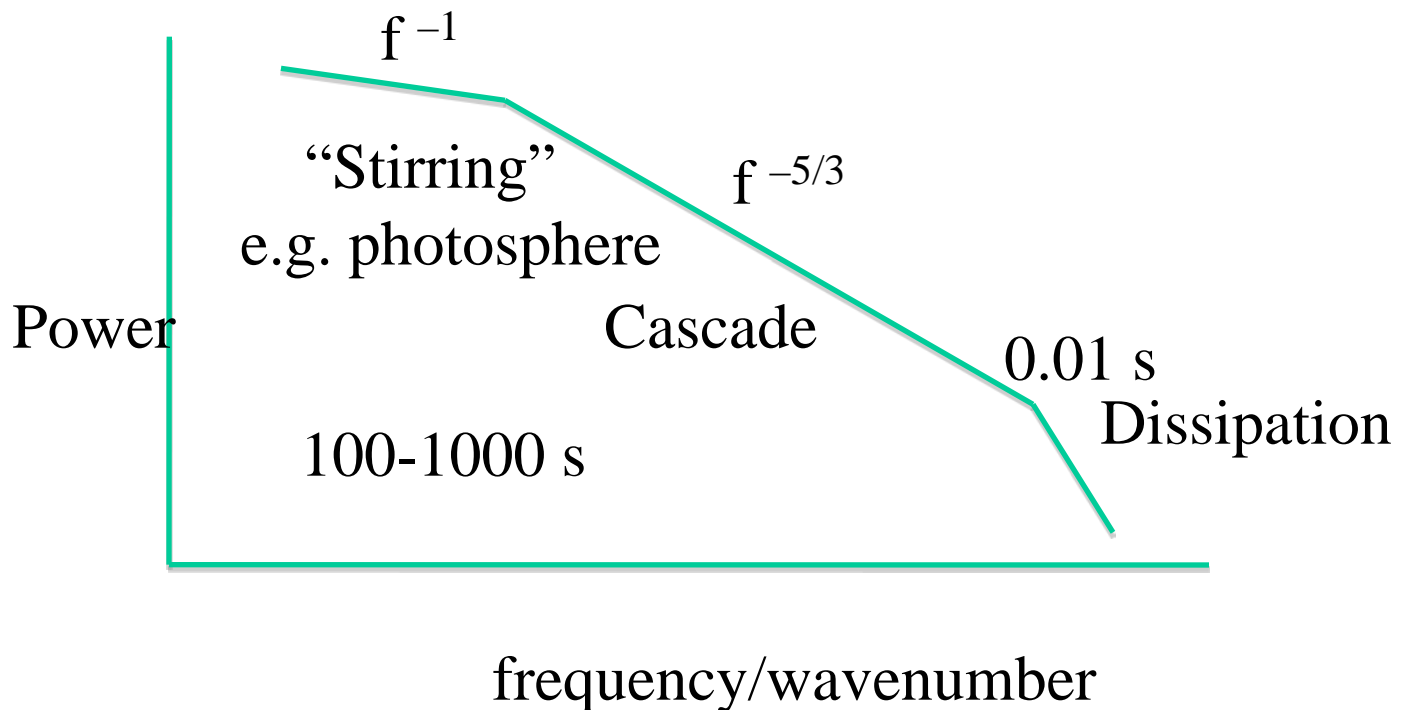
$$= \frac{1}{v^2} \frac{\partial}{\partial v} \left(v^2 D_{vv} \frac{\partial f_s}{\partial v} \right) - \frac{(1-\mu^2)^{1/2}}{v^2} \frac{\partial}{\partial v} \left(v D_{v\mu} \frac{\partial f_s}{\partial \mu} \right) - \frac{1}{v} \frac{\partial}{\partial \mu} \left((1-\mu^2)^{1/2} D_{\mu v} \frac{\partial f_s}{\partial v} \right) + \frac{1}{v^2} \frac{\partial}{\partial \mu} \left((1-\mu^2) D_{\mu\mu} \frac{\partial f_s}{\partial \mu} \right)$$



MHD Turbulence

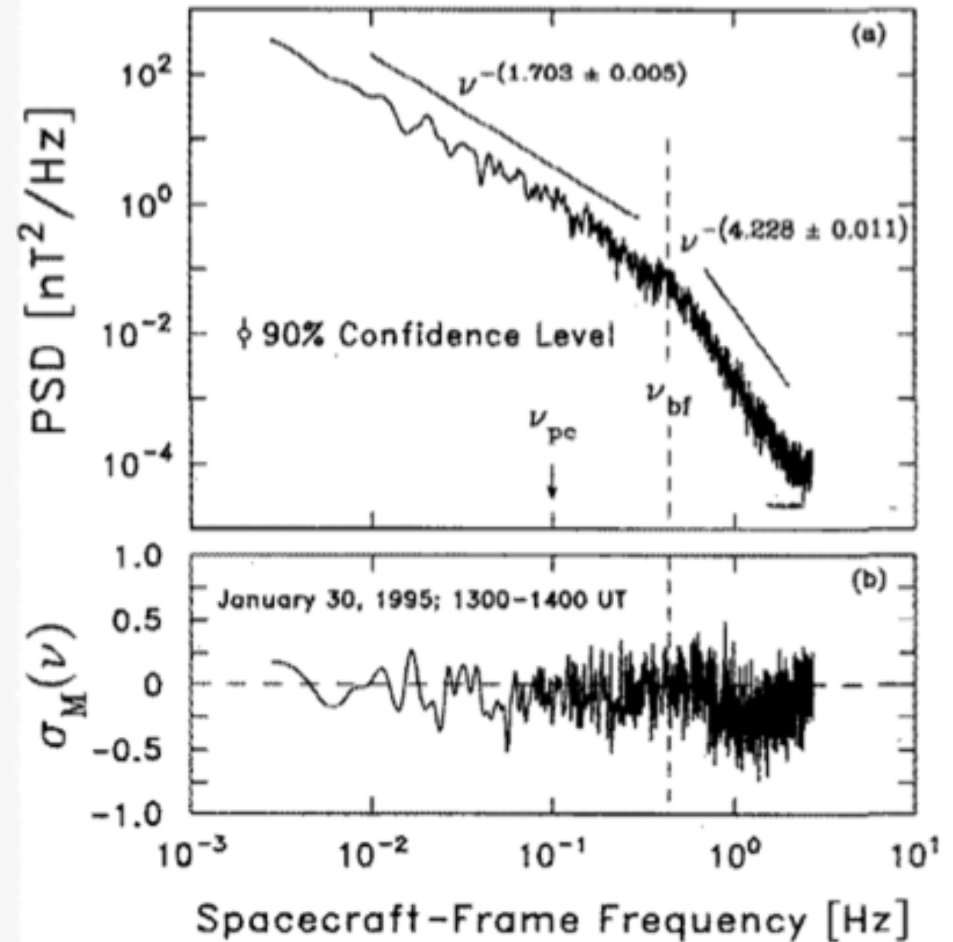
Alfvén waves are difficult to damp ...

Dissipation of the waves by turbulence;
cyclotron resonance and/or Landau damping





A solar wind power spectrum showing the inertial and “dissipation” range.

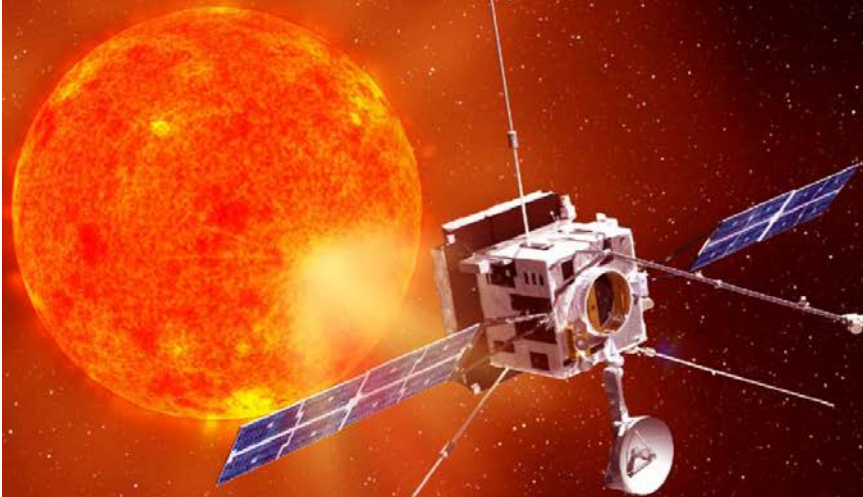


R. J. Leamon, C. W. Smith, N. F. Ness, W. H. Matthaeus, H. K. Wong, *J. Geophys. Res.*, 103, 4775, 1998.



Solar Orbiter

The future:



Exploring the Sun-Earth connection

Solar Orbiter

**A high-
resolution
mission to
the Sun and
inner
heliosphere**

ESA

2017



Solar Probe Plus



APL

Solar Probe Plus

A NASA Mission to Touch the Sun





Summary

- **Coronal imaging and spectroscopy as of in-situ observations indicate strong deviations of the plasma from thermal equilibrium**
- **Semi-kinetic particle models with self-consistent wave spectra provide valuable physical insights**
- **Such models describe some essential features of the observations of the solar corona and solar wind**
- **But the thermodynamics of the solar corona and solar wind requires a fully-kinetic approach**
- **Turbulence transport as well as cascading and dissipation in the kinetic domain are not yet fully understood**



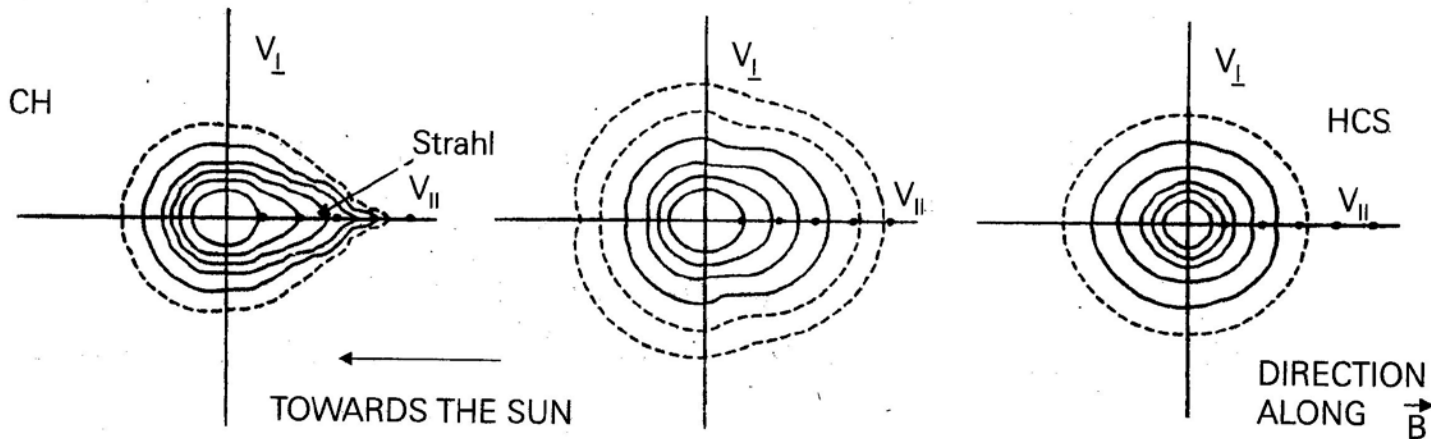
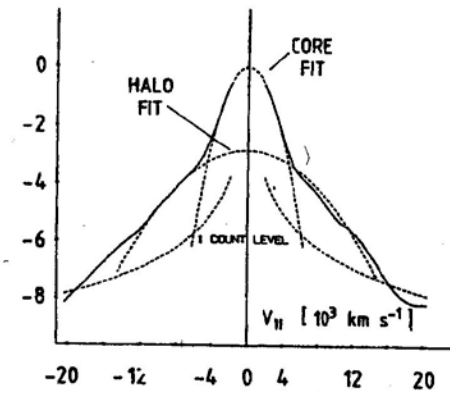
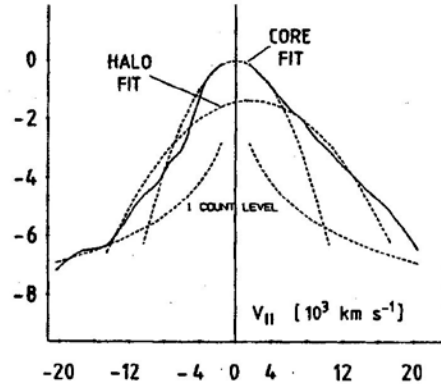
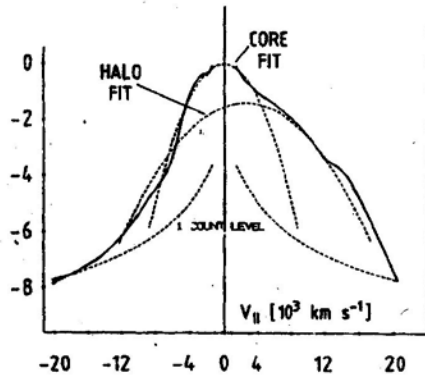
Thanks!
Gracias!
Obrigado!



Solar Wind Electrons: Non-Thermal Distributions

$$T_e = 1-2 \cdot 10^5 \text{ K}$$

Log (F/_{MAX})



Pilipp et al., JGR, 92, 1075, 1987

Core (96%), halo (4%) electrons, and „strahl“



How do radial field inversions vary with distance? In situ process or remnant of heating-acceleration?

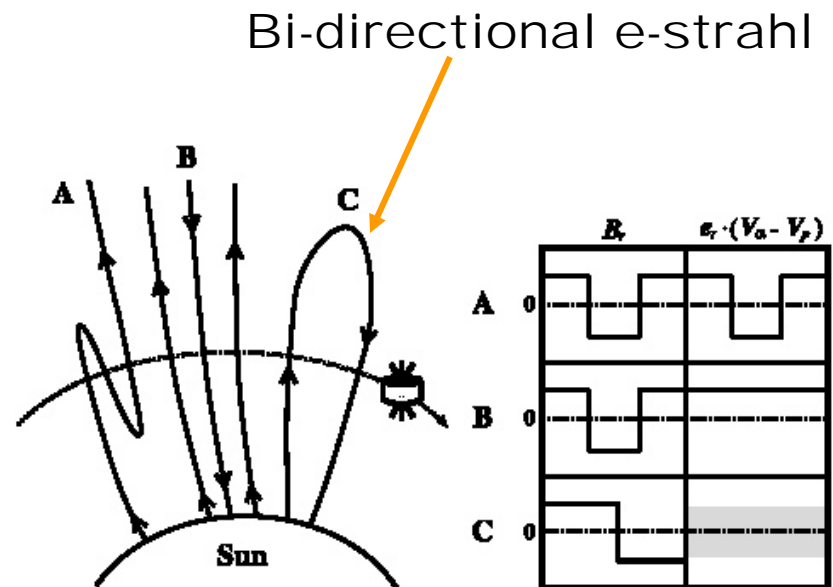
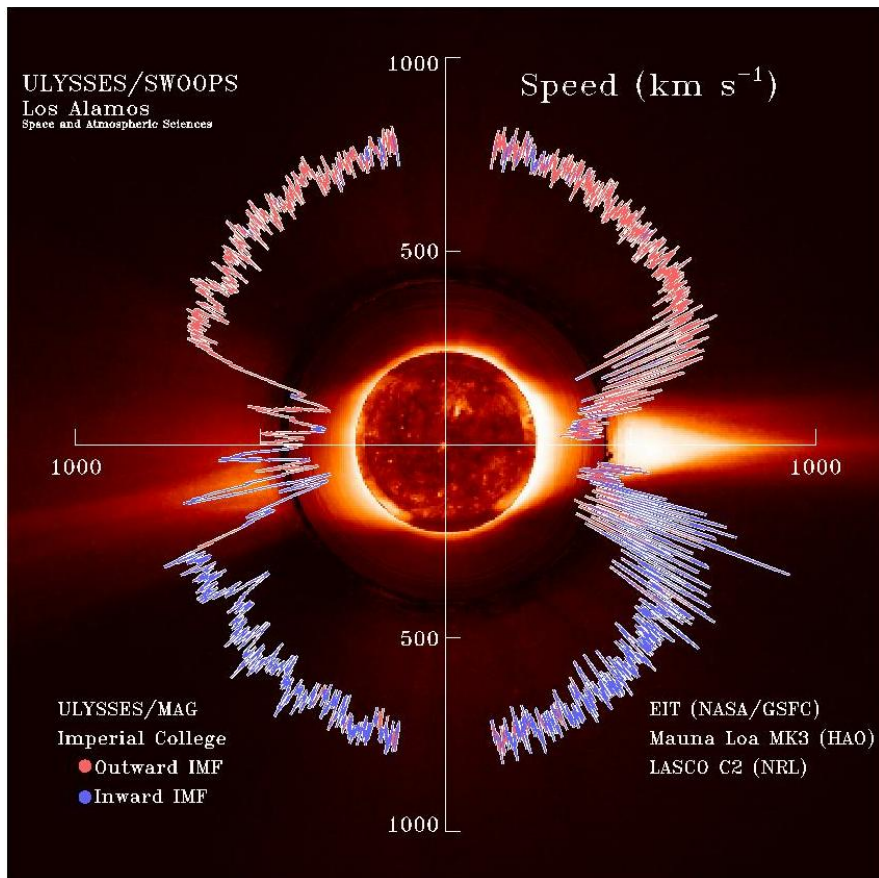


Figure 1. (left) Cartoon of three possible configurations across discontinuities in the radial magnetic field. (right) Diagrams of the variation in radial magnetic field strength and alpha particle-proton differential streaming in the radial direction across the three classes of discontinuities.